

University of Kentucky

UKnowledge

---

Theses and Dissertations--Electrical and  
Computer Engineering

Electrical and Computer Engineering

---

2018

## CONTRIBUTIONS TO HYBRID POWER SYSTEMS INCORPORATING RENEWABLES FOR DESALINATION SYSTEMS

Nasser Alawhali

*University of Kentucky*, [nasser.alawhali@uky.edu](mailto:nasser.alawhali@uky.edu)

Digital Object Identifier: <https://doi.org/10.13023/ETD.2018.124>

[Right click to open a feedback form in a new tab to let us know how this document benefits you.](#)

### Recommended Citation

Alawhali, Nasser, "CONTRIBUTIONS TO HYBRID POWER SYSTEMS INCORPORATING RENEWABLES FOR DESALINATION SYSTEMS" (2018). *Theses and Dissertations--Electrical and Computer Engineering*. 115. [https://uknowledge.uky.edu/ece\\_etds/115](https://uknowledge.uky.edu/ece_etds/115)

This Master's Thesis is brought to you for free and open access by the Electrical and Computer Engineering at UKnowledge. It has been accepted for inclusion in Theses and Dissertations--Electrical and Computer Engineering by an authorized administrator of UKnowledge. For more information, please contact [UKnowledge@lsv.uky.edu](mailto:UKnowledge@lsv.uky.edu).

## **STUDENT AGREEMENT:**

I represent that my thesis or dissertation and abstract are my original work. Proper attribution has been given to all outside sources. I understand that I am solely responsible for obtaining any needed copyright permissions. I have obtained needed written permission statement(s) from the owner(s) of each third-party copyrighted matter to be included in my work, allowing electronic distribution (if such use is not permitted by the fair use doctrine) which will be submitted to UKnowledge as Additional File.

I hereby grant to The University of Kentucky and its agents the irrevocable, non-exclusive, and royalty-free license to archive and make accessible my work in whole or in part in all forms of media, now or hereafter known. I agree that the document mentioned above may be made available immediately for worldwide access unless an embargo applies.

I retain all other ownership rights to the copyright of my work. I also retain the right to use in future works (such as articles or books) all or part of my work. I understand that I am free to register the copyright to my work.

## **REVIEW, APPROVAL AND ACCEPTANCE**

The document mentioned above has been reviewed and accepted by the student's advisor, on behalf of the advisory committee, and by the Director of Graduate Studies (DGS), on behalf of the program; we verify that this is the final, approved version of the student's thesis including all changes required by the advisory committee. The undersigned agree to abide by the statements above.

Nasser Alawhali, Student

Dr. Dan M. Ionel, Major Professor

Dr. Caicheng Lu, Director of Graduate Studies

CONTRIBUTIONS TO HYBRID POWER SYSTEMS INCORPORATING  
RENEWABLES FOR DESALINATION SYSTEMS

---

THESIS

---

A thesis submitted in partial fulfillment  
of the requirements for the degree of  
Master of Science in Electrical  
Engineering in the College of Engineering  
at the University of Kentucky

By

Nasser Alawhali  
Lexington, Kentucky

Director: Dr. Dan M. Ionel, Professor and L. Stanley Pigman Chair in Power  
Lexington, Kentucky 2018

Copyright© Nasser Alawhali 2018

## ABSTRACT OF THESIS

### CONTRIBUTIONS TO HYBRID POWER SYSTEMS INCORPORATING RENEWABLES FOR DESALINATION SYSTEMS

Renewable energy is one of the most reliable resource that can be used to generate the electricity. It is expected to be the most highly used resource for electricity generation in many countries in the world in the next few decades. Renewable energy resources can be used in several purposes. It can be used for electricity generation, water desalination and mining. Using renewable resources to desalinate the water has several benefits such as reduce the emission, save money and improve the public health. The research described in the thesis focuses on the analysis of using the renewable resources such as solar and wind turbines for desalination plant. The output power from wind turbine is connected through converter and the excess power will be transfer back to the main grid. The photo-voltaic system (PV) is divided into several sections, each section has its own DC-DC converter for maximum power point tracking and a two-level grid connected inverter with different control strategies. The functions of the battery are explored by connecting it to the system in order to prevent possible voltage fluctuations and as a buffer storage in order to eliminate the power mismatch between PV array generation and load demand. Computer models of the system are developed and implemented using the *PSCAD<sup>TM</sup>/EMTDC<sup>TM</sup>* software.

KEYWORDS: Renewable, Desalination, Energy Storage, Wind, Power.

Author's signature: Nasser Alawhali

Date: 04/18/2018

CONTRIBUTIONS TO HYBRID POWER SYSTEMS INCORPORATING  
RENEWABLES FOR DESALINATION SYSTEMS

By  
Nasser Alawhali

Director of Thesis: Dr. Dan M. Ionel

Director of Graduate Studies: Dr. Caicheng Lu

Date: 04/18/2018

## *DEDICATION*

*Dedicated to my lovely parents, my wife and everyone  
supports and encourages me  
for their infinite support, love, following up and  
encouragement*

## ACKNOWLEDGEMENTS

First of all, I would like to express my appreciation to my supervisor Dr. Dan. M. IoneL for his supports, advises, encouragement and mentoring during my courses studies and research. Also, I would like to thank him for giving me the opportunity to become a graduate student under his supervision and work in the SPARK laboratory at university of KENTUCKY. I also, wish to thank Dr. Vandana Rallabandi, who supports me and made a time to assist me with the design and simulation of my research.

I am also very thankful for Dr. Aaron M. Cramer and Dr. Yuan Liao for their review and input as members of my thesis committee. Also, I would like to thank them for everything I learned from all classes I have taken with them during my studies.

Also my colleagues and friends at SPARK Lab, with whom it has been wonderful to work with. I am very grateful to my lovely wife Mrs. Sarah Alfadel, who supports me and always made a time for me to focus on my research. Last but not the least, I would like to make a special thanks for my parents, who have supported and encouraged me from the first day I left my home country. No words could explain my deep appreciation for them. Without them, I would not be able to do anything.

Nasser Alawhali  
, 2018

# Contents

<b>ACKNOWLEDGEMENTS</b>	<b>iii</b>
<b>List of Figures</b>	<b>vii</b>
<b>List of Tables</b>	<b>xiii</b>
<b>1 Introduction</b>	<b>1</b>
1.1 Research background . . . . .	3
1.2 Thesis outline . . . . .	4
<b>2 Modeling of Components and Subsystems</b>	<b>6</b>
2.1 Introduction . . . . .	6
2.2 Problem formulated . . . . .	7
2.3 Desalination systems . . . . .	9
2.3.1 Thermal and membrane based methods . . . . .	9
2.3.2 Typical power system requirements and ratings . . . . .	11
2.4 Photovoltaic cells and arrays . . . . .	14
2.4.1 PV output characteristics . . . . .	16
2.4.2 PV module and array setup . . . . .	18
2.4.3 MPPT . . . . .	21
2.4.4 Converters and electric machines . . . . .	23
2.5 Wind turbine . . . . .	26

2.5.1	Wind turbine characteristics . . . . .	26
2.5.2	Wind turbine controllers . . . . .	34
2.5.3	Permanent magnet synchronous generator model . . . . .	36
2.5.4	PSCAD model . . . . .	39
<b>3</b>	<b>Simulation of PV, Wind Turbine, Water Desalination Plant and the Grid</b>	<b>44</b>
3.1	Introduction . . . . .	44
3.2	PV System . . . . .	47
3.2.1	PV array . . . . .	47
3.2.2	MPPT . . . . .	50
3.3	Wind turbine . . . . .	51
3.3.1	AC/DC/AC converters . . . . .	53
3.3.2	Phase locked loop . . . . .	57
3.3.3	Output power control . . . . .	60
3.4	Water desalination plant . . . . .	61
3.5	Simulation results and discussion . . . . .	62
3.6	Summary . . . . .	65
<b>4</b>	<b>Case Studies for Desalination Plant Integrated with Hybrid Power System</b>	<b>73</b>
4.1	Introduction . . . . .	73
4.2	Overall rating . . . . .	74
4.2.1	Simulation results . . . . .	76
<b>5</b>	<b>Conclusions and Future Work</b>	<b>85</b>
5.1	Conclusions . . . . .	85
5.2	Future work . . . . .	86

References	88
Vita	94

# List of Figures

2.1	Growth in U.S. Wind Energy Installations [1]. . . . .	8
2.2	MSF process [2] . . . . .	10
2.3	MED process [3] . . . . .	10
2.4	Solar radiation data [4] . . . . .	15
2.5	Equivalent circuit of PV cell [5]. . . . .	16
2.6	PV cell configuration from solar cell to solar array [6]. . . . .	19
2.7	IV curve of PVs arrays with different configurations [7]. . . . .	20
2.8	Solar Cell I-V Characteristic Curve [8]. . . . .	22
2.9	Circuit implementation in PSCAD for DC/DC converter (a) buck, (b) boost , (c) buck-boost and (d) Cuk [9]. . . . .	24
2.10	The components of the wind turbine [10]. . . . .	27
2.11	(a) Fixed-speed wind turbine, (b) partial variable speed wind turbine with variable rotor resistance [11]. . . . .	28
2.12	(a) Fixed-speed wind turbine, (b) partial variable speed wind turbine with variable rotor resistance [11]. . . . .	28
2.13	(a) Two level back to back converters with passive rectifier, (b) Two-level back-to-back converters with active rectifier [12]. . . . .	29
2.14	Block diagram of variable-speed SG wind energy system [13]. . . . .	30
2.15	Wind power VS wind speed curve [13]. . . . .	31
2.16	An example of theoretical power production against rotor's diameter change for small wind turbines at wind speed 10 m/s [14]. . . . .	32

2.17	Power coefficient $C_p$ as a function of TSR $\lambda$ and pitch angle in degrees.	34
2.18	PS-CAD Model of a wind turbine generator. . . . .	43
3.1	Schematic of grid tied PV system consists of multiple units connected in parallel with one transformer [9]. . . . .	46
3.2	The schematic of grid tied wind turbine system including a wind turbine connected with one PMSG, converters and transformer. . . . .	46
3.3	Schematic of PV unit in PSCAD showing the solar PV panel, 2-level inverter, DC-DC converter, transformer and grid based on [9]. . . . .	48
3.4	Solar panel I-V characteristics curve [9]. . . . .	49
3.5	Schematic diagram for MPPT control in the PSCAD [9]. . . . .	51
3.6	Control diagram for DC-DC converter in the PSCAD [9]. . . . .	51
3.7	Schematic of 2MW wind turbine unit in PSCAD showing the turbine, mechanical dynamic block, PMSG, AC-DC converter, DC-AC converter and transformer. . . . .	52
3.8	Schematic diagram for the control system of the conversion system. . . . .	54
3.9	Scematic diagram for the rectifier control based on [15]. . . . .	55
3.10	Scematic diagram for the inverter control based on [15]. . . . .	55
3.11	Power circuit diagram in PSCAD simulator shows the control system that are used for the converters. . . . .	56
3.12	Power circuit diagram in PSCAD simulator shows the phase locked loop that are used to track the grid voltage. . . . .	58
3.13	Power circuit diagram in PSCAD simulator shows 2-level inverters, 2-level rectifier and the control system for both the rectifier and the inverter. . . . .	59
3.14	The structure of the phase locked loop PLL [16]. . . . .	59

3.15	Power circuit diagram in PSCAD simulator shows the 2-level converter used for rotor side and grid side. . . . .	61
3.16	(a) Overall Schematic diagram diagram in PSCAD for wind farm connected with the grid, (b) Detail schematic inside the wind farm showing six wind turbine units connected in parallel with total of 12 MW. The detail model of each unit is illustrated in fig 3.7 . . . . .	64
3.17	The wind speed and the mechanical speed of the generator, where the mechanical speed equal 0.8 p.u. at wind speed 9.5 m/s and drops to 0.65 p.u. when the wind speed suddenly changed. . . . .	65
3.18	The output active and reactive powers from one wind turbine, where numeric change happens in the first second and then being regulated by the controller. When the wind speed suddenly changed, the output active power drops to 0.65 pu and the reactive power drops to 0.01 pu since the active power depends on the wind speed. . . . .	66
3.19	The total output active and reactive powers from six wind turbine to the grid. . . . .	66
3.20	The three phase output voltages from six wind turbines. . . . .	67
3.21	The three phase output currents from six turbines, where it decreases when the wind speed decrease. . . . .	68
3.22	The output voltage of the rectifier, which maintains the voltage at 1.1 kV. While the wind speed suddenly decreases from 9.5 m/s to 7.5 m/s at 20s, the rectifier maintains the voltage at at the same value with a numeric change due to the change in $I_q$ . . . . .	69
3.23	The $I_d$ , $I_q$ and their reference currents for the controller of rectifier, where the $I_d$ is set to be zero and the $I_q$ is regulated to maintain the voltage at reference value. . . . .	70

3.24	The $I_d$ , $I_q$ and their reference currents for the controller of inverter, where the $I_d$ is set to be zero and the $I_q$ is regulated to maintain the active power. . . . .	71
4.1	(a) Schematic of the system in PSCAD showing the wind farm connected in parallel with 1 MW solar plant, (b) Six wind turbine units connected in parallel with total of 12 MW. . . . .	75
4.2	Schematic of the system in PSCAD showing the PV system with power controlling based on [9]. The detail model is illustrated in fig3.3 . . .	76
4.3	(a) Schematic of the system in PSCAD showing the load connected with the wind farm, which consists of 6 wind turbines connected in parallel with total of 12 MW, (b) Six wind turbine units connected in parallel with total of 12 MW. . . . .	77
4.4	The output active and reactive powers from one wind turbine, where numeric change happens in the first second and then being regulated by the controller. When the wind speed suddenly changed, the output active power drops to 0.65 pu and the reactive power drops to 0.01 pu since the active power depends on the wind speed. . . . .	78
4.5	The output active and reactive powers from six wind turbines and PV system, where numeric change happens in the first second and then being regulated by the controller. When the wind speed suddenly changed, the output active power drops to 5 MW and the reactive power drops to 0.01 pu since the active power depends on the wind speed. . . . .	79

4.6	The output active and reactive powers from one wind turbine, where numeric change happens in the first second and then being regulated by the controller. When the wind speed suddenly changed, the output active power drops to 0.65 pu and the reactive power drops to 0.01 pu since the active power depends on the wind speed. . . . .	79
4.7	The DC Power from the PV. Reduction in irradiance at 20s simulation time leads to decrease in PV output current making the PV DC power drop. . . . .	80
4.8	PV AC power output at unity power factor irrespective of changes in array irradiance.. . . . .	80
4.9	The three phase output voltages of the system. . . . .	81
4.10	The three phase output currents to the grid. . . . .	81
4.11	The control system of the power conversion system of the wind turbine operating in the stand-alone mode. . . . .	82
4.12	The $I_q$ current and its reference current for the controller of inverter, where the $I_d$ is set to be zero and the $I_q$ is regulated to maintain the active power. The magnitude of the $I_q$ current is high, because the rating of the system, where the control is being difficult for high ratings.	82
4.13	The $I_d$ current and its reference current for the controller of inverter, where is set to be zero and the. The high ripple is a result of the PI tuning of the controller and the high rating of the system. . . . .	83
4.14	The output active and reactive powers from the system, where numeric change happens in the first second and then being regulated by the controller. When the wind speed and the irradiance suddenly changed, the output active power drops to 5.1 MW and the reactive power drops to 0.01 pu since the active power depends on the wind speed. . . . .	83

4.15 Schematic of the system in PSCAD showing the wind farm connected in parallel with solar plant. The wind farm consists of 6 wind turbine units connected in parallel with total of 12 MW and the PV rated of 1 MW. . . . .	84
4.16 Schematic of the system in PSCAD showing the wind farm connected in parallel with solar plant. The wind farm consists of 6 wind turbine units connected in parallel with total of 12 MW and the PV rated of 1 MW. . . . .	84

# List of Tables

2.1	PV materials efficiencies . . . . .	15
2.2	Generator data . . . . .	41
2.3	The wind turbine parameters. . . . .	41
2.4	The wind governor parameters. . . . .	42
2.5	The synchronous generator parameters. . . . .	42
3.1	PV cell and module specifications . . . . .	50
3.2	Electrical specification of the generator . . . . .	53

# Chapter 1

## Introduction

The electric power generated from wind turbines has increased over the past few decades. Using the wind power has many benefits. For instance, it is clean energy, which is friendly for the environment. In addition, it is cost effective being one of the cheapest energy resources available today [17]. Wind power start to become a popular resource for electricity generation across the USA due to its costs and the distribution of wind resources wind energy can be divided to into different categorized based on its size. There are large wind turbines, which are used to generate a large number of megawatts; there are also small wind turbines, which usually produce no more than 100 kilowatts of electricity [18]. In addition, these can be installed at home, small business and farms. A very small wind turbines, which produce about 50 watts and can be used to charge batteries and power small motors [19]. Solar power also is one of the fastest growing renewable energy resources in the last decade. PV has several

important characteristics in term of environment, installation and cost. It is suitable for areas such as residential, industrial, commercial and it can expand its power utilities capacity. In addition, since it depends on the sunlight, it is friendly to the environment and has a little effect on it. Batteries in PV systems could be beneficial for some systems, which stores the energy during the daytime in batteries and feed the grid after the sunshine. The capacity of a battery counts on the discharge current, temperature and other factors, which makes the electrochemical devices counts on a large number of material properties meeting a defined standard to function correctly [20]. Global demand for clean water continues to increase since the world population increases and the water's resources are becoming scarce. Countries around the world struggle from the scarce resources of the water they have. Therefore, national plans has been developed in order to use the seawater to cover the needs for freshwater. Furthermore, desalinate became one of the most popular ways to achieve these objectives [3]. However, the desalination process is consuming substantial energy, which could be an obstruction for countries that have limited energy resources. Power electronics conversion system provides an interface that enables flexible interconnection of different systems such as renewables, batteries and controllable loads to the grid [21].

## 1.1 Research background

Extracting the maximum power from the wind turbine has been the focus of a large amount of research in recent years with applying new control strategies for higher efficiency. Some research have explained several type of control strategies for aerodynamic design of the turbine blades [22], some researchers focus on the control technologies of the generator, which can be employed to extract the maximum power from the turbine. Pitch control strategy can be used to maintain the optimal power from the turbine over a wide range of wind speed conditions [23, 24]. For low wind speed, the desired generator torque and the resulting rotor speed were controlled in order to operate the wind turbine close to maximum efficiency [25]. Researchers have proposed a significant amount of researches on control technologies of power conversion system of the wind turbine [25, 26]. Different type of machines could be used for wind turbines in order to transfer the mechanical power to electrical power and connected with the grid such as squirrel-cage induction generator SCIG, wound rotor induction generators WRIG, doubly fed induction generator DFIG and permanent magnet synchronous generator PMSG. PMSG has higher efficiency and better performance compare to the other types of generators. Also, it can be used without a gearbox, which results to reduction of the weight of the nacelle and costs [27]. Wind energy have been incorporated with different renewable energy resources such as PV system. Also, PV-hybrid system is suitable for stand alone applications.

Water desalination process is an intensive energy consumption, which results to high cost. Thermal process requires thermal and electrical energy for water desalination process such as driving the cooling pumps, recycling pumps and brine blow down pumps.

## **1.2 Thesis outline**

Chapter 1 introduces the research background for wind energy, PV systems and the parameters to be considered for design. To refine the main goals of the research, literature reviews of wind energy and control strategies are covered in this chapter.

Chapter 2 discusses the modeling of components and subsystems and gives an overview of the technologies and developments in control systems of the wind energy , water desalination process from an electrical view and the PV cell design and control.

Chapter 3 explains the configuration and associated control methods of a multi-megawatts grid connected wind farm. The wind farm consists of several wind turbine units connected in parallel and integrated with the grid in order to observe the steady state and transient effect with changes in wind speeds and environment parameters.

Chapter 4 presents several case studies of grid integrated with wind farm, PV system and water desalination plant. A control strategy for stand alone system is also introduced.

Chapter 5 concludes the research with a brief summary of original contributions

and work. Also, suggestions for future work that can be extended based on the current research was explained.

# Chapter 2

## Modeling of Components and Subsystems

### 2.1 Introduction

This chapter introduces the water desalination systems, their main components and operational principles. In addition, it introduces the PV cells and arrays and the very important concept of maximum power point tracking (MPPT). Wind turbines characteristics and the need design for integration with the electric grid are also explained. Furthermore, the power electronic devices and functions needed for both DC-AC and DC-DC conversion are also introduced.

Global demand for clean water continues to increase since the world population increases and the water's resources are becoming scarce. Countries around the world struggle from the scarce resources of the water they have. Therefore, national plans has been developed in order to use the seawater to cover the needs for freshwater.

Furthermore, desalinate became one of the most popular ways to achieve these objectives. However, the desalination process is consuming substantial energy, which could be an obstruction for countries that have limited energy resources [3].

The electric power generated from wind turbines has increased over the past few decades. Using the wind power has many benefits. For instance, it is clean energy, which is friendly for the environment. In addition, it is cost effective being one of the cheapest energy resources available today. Wind power start to become a popular resource for electricity generation across the USA due to its price and the distribution of wind resources. According to [19], wind power has become the fastest growing energy resource in the industry of energy. As show in Fig 2.1, wind power installation have significantly increased in the us. With an accelerated growth taking place since 2011 [1]. The technology and researches of wind turbine has come a way since the crisis of energy that happened in 1970s [20].

## **2.2 Problem formulated**

The thesis mainly describes and focuses on the analysis of using the hybrid power system incorporating renewable resources such as solar and wind turbines for desalination plant. The wind turbines are divided into multi-megawatt units and each turbine has its own power conversion system, control system for maximum power point and transformer. The output power from wind turbine is connected through converter and

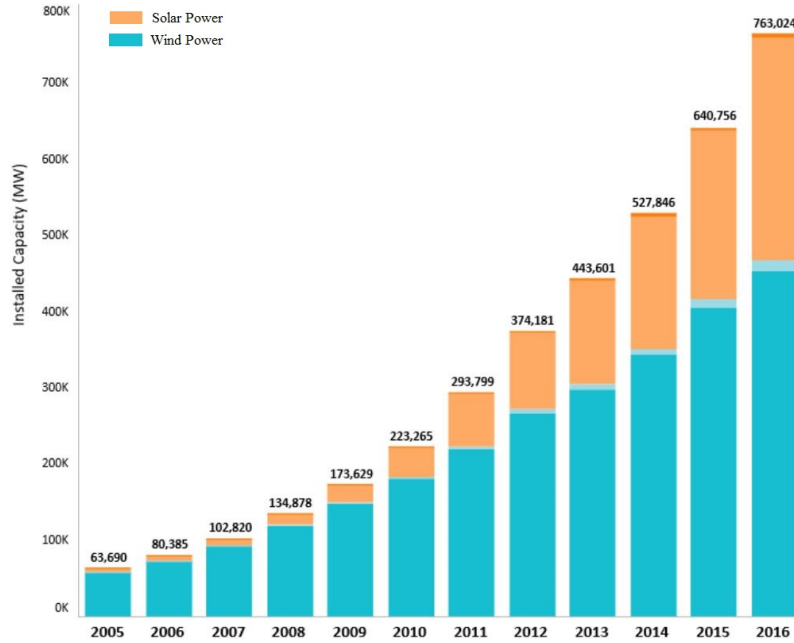


Figure 2.1: Growth in U.S. Wind Energy Installations [1].

the excess power will be transfer back to the existing grid. The photo-voltaic system (PV) is divided into several sections, each section has its own DC-DC converter for maximum power point tracking and a two-level grid connected inverter with different control strategies. The load in the thesis will be a water desalination plant, since the process of water desalination is an intensive energy consumption, which is a proper load for the system. Different simulation conditions will be introduced in order to ensure that the control system for both the wind turbines and PV system is working and producing the maximum power from the system. The entire system will be integrated with with a reliable grid, which ensure that the water desalination plant will be operated all the day regardless the wind speed. In addition, the functions of the

wind farm and the PV system are explored by connecting it to the load and work as stand alone mode in order to prevent the power outage on the load, where it should work all the day. Computer models of the system are developed and implemented using the *PSCAD<sup>TM</sup>/EMTDC<sup>TM</sup>* software.

## **2.3 Desalination systems**

### **2.3.1 Thermal and membrane based methods**

Water can be desalinated using different methods. The most popular technologies are thermal and membrane method. Firstly, thermal desalination method, which use the heat to vaporize the fresh water. In addition, the process includes multistage flash (MSF), vapor compression (VP), low temperature evaporation (LTE) and multiple-effect desalination (MED). Moreover, all of these process condense the steam to supply the heat that is needed to evaporate the water. This method is mostly use in industrial process applications since it produces high purity water. In the MSF process, the sea water is heated to about 90-120C using the heat of condensation of the vapor and then flash at decreasing levels of pressure and finally condensed and recovered as fresh water as shown in fig 2.2 [3].

In MED process, there are two main stage. The first one is heated by low pressure steam, which is about 0.3 bar. Therefore, vapors will be produced and directed to the second stage and be as the heat source. In the first stages, vapor passes through

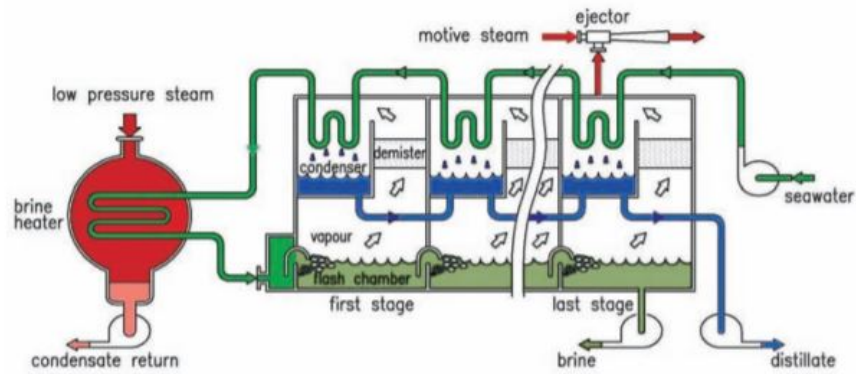


Figure 2.2: MSF process [2]

the demisters to next stage. Moreover, vapor from the second stage is condensed by using the sea water as the coolant. Fig 2.3 illustrates the MED process. MES process are being popular since the low grade heat, low energy consumption and waste heat utilization [2].

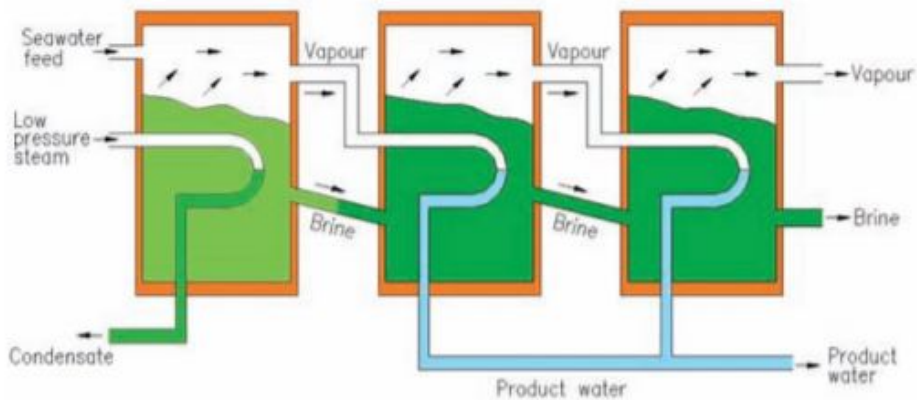


Figure 2.3: MED process [3]

Secondly, membrane desalination method, which use the high pressure generated from electrical pump to separate the fresh water from the saline water.

### 2.3.2 Typical power system requirements and ratings

Water desalination process is an intensive energy consumption, which results to high cost. Thermal process such as multistage flash (MSF) requires thermal and electrical energy for water desalination process. It requires the electrical energy for driving the pumps such as water cooling pumps, water recycling pumps and brine blow down pumps [2]. It mainly consumes between  $19.58 \text{ kWh}/m^3$  and  $27.25 \text{ kWh}/m^3$  to desalinated water. On the other hand, reverse osmosis (RO) requires electrical energy for the high pressure pumps, which consumes about  $4\text{-}6 \text{ kWh}/m^3$ , which make it widely used in many of the desalination plants [54]. Furthermore, 63.7 % of the total capacity of the desalinated water is produced by membrane process, while 34.3 % is produced by thermal process [2, 28]. Therefore, using the renewable energy resources for the water desalination could be an energy saving. Renewable energy resources can be divided to main categories. First, dispatchable resources such as biomass, hydro, geothermal and concentrated solar power with storage. Second, non-dispatchable resources such as ocean power resource, wind and solar photovoltaic. It is also known as variable renewable energy (VRE). The minimum energy requirement for water desalination can be expressed by using Van't Hoff formula as following:

$$\pi = cRT, \quad (2.1)$$

Where,  $\pi$  the osmotic pressure,  $c$  the molar concentration of salt ions,  $R$  the

gas constant, which equals 0.082 and  $T$  the ambient temperature on the absolute temperature scale. For the seawater,  $c$  equals 1.128 mol/liter, which results the  $\pi$  to be 27.8 bar or 278 kg.m/L. Moreover, since each 10 Joules equal 1 kg.m or 0.77 kWh/ $m^3$ , which is the minimum theoretical energy requirement [3].

Integrate the VRE with the electric power grid requires several measurements in order to protect the stability of the grid. Firstly, variability that caused by temporal availability of the resources. Secondly, uncertainty due to sudden changes in the resource availability. Thirdly, location properties due to the geographical changes. Finally, low marginal cost since the renewable resources are freely available. Furthermore, the impact on voltage variation and power system protection's behavior under faults conditions should be considered [3].

Energy storage can be beneficial for the system. In addition, it is needed to save the exceed energy production. For instance, solar energy can be stored during the day time to use it after the sunset. Moreover, energy storage improves the reliability and stability of the grid. Energy can be stored by conversion of the electricity into different form of energy. For instance, pumped storage hydro, where compressed air energy storage. Another example by using electric batteries which charge during the availability of the energy then use it to supply the system when the source of the energy is not available [3].

wind energy can be divided to into different categorized based on its size. Large

wind turbines, which are used to generate a large number of megawatts. Moreover, it can be used to power hundreds of buildings. Small wind turbines, which usually produce no more than 100 kilowatts of electricity. In addition, it can be installed at home, small business and farms. Finally, very small wind turbines, which produce about 50 watts and can be used to charge batteries and power small motors [2].

The output power generated by wind turbines mainly depends on the wind speed, where it should be strong in order to generate a high output power. Therefore, integrate the wind farm with grid or connect the wind farm with a load as stand alone system should ensure the reliability of the system and voltage stability. In addition, the PV system mainly depends on the solar radiation and the temperature. Thus, integrate the PV system with the grid without an energy storage such as a battery should not affect the system reliability after the sunshine, where the produced power from the PV will be zero. In this model, the load will be a water desalination plant with 1 MW rating. Therefore, the output power from the entire system includes the wind farm and the PV system at every conditions should be higher than the load rating to ensure that the water desalination plant works all the day regardless the changes in the wind speeds and the solar irradiation. Thus, the wind farm consists of 6 wind turbines connected in parallel with total of 12 MW and the PV system rating is 1 MW. Any change in the wind speed should not affect the reliability of the system, where the load requires 1 MW. Furthermore, since there is no energy storage

associated with the system such as a battery, the wind farm must feed the load after the sunshine where the output power from the PV will be zero and the load is 1 MW.

## 2.4 Photovoltaic cells and arrays

Photovoltaic (PV) system mainly converts the sunlight into electricity. It is used in different industries around the world. Solar power is one of the fastest growing renewable energy resources in the last decade. PV has several important characteristics in terms of environment, installation and cost. It is suitable for areas such as residential, industrial, commercial and expanding of power utilities capacity. In addition, since it depends on the sunlight, it is friendly to the environment and has a little effect on it. Moreover, the installation of PV system is not difficult since it has no moving parts to wear out. Therefore, these benefits make the PV system desirable in many industries. Temperature has a significant effect on the efficiency of the PV cell, which short circuit current increases when the temperature increases [29]. One of the most suitable places for PV system is Saudi Arabia since the high solar potential. For instance, while the average annual rate of solar radiation is 100-200 W/m<sup>2</sup> in most of the high concentrated solar areas, it is about 250 W/m<sup>2</sup> in Saudi Arabia. In addition, the average sunshine hours in Saudi Arabia is 8.89 hours and it is a rainless country, which means the sun is available most of the year. It is planned to generate 54 GW from renewable resources by 2032 and about 70 percent of this capacity would be

from solar. Fig 2.4 illustrates a daily and monthly solar radiation in Makkah,western area of Saudi Arabia. It ranges between 4.15 kWh/m<sup>2</sup>/day and 7.17 kWh/m<sup>2</sup>/day. Moreover, the solar irradiance is high during the summer months which start from March to September. On the other hand it is low in the winter months which start from October to February [4].

Table 2.1: PV materials efficiencies

Material	Typical Efficiencies
Gallium arsenide (GaAs)	20
Monocrystalline silicon	14 to 17
Polycrystalline silicon	11.5 to 14
Ribbon Silicon	11 to 13
Copper indium gallium selenide (CIGS)	9 to 11.5
Cadmium telluride (CdTe)	8 to 10
Amorphous silicon (a-Si)	5 to 9.5
Graetzel	4 to 5
Polymer	1 to 2.5

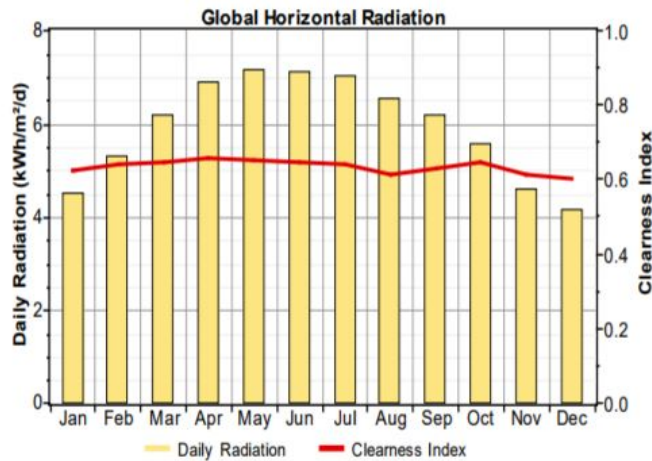


Figure 2.4: Solar radiation data [4]

### 2.4.1 PV output characteristics

Photovoltaic cell is mainly represented by the simple double exponential circuit as shown in fig 2.5. In addition, it is systematized by one power supply and two diode, where the power supply converts the solar radiation into photo current  $I_{ph}$  and diodes D1 and D2 and resistances regulate the current that flows to the load [30].

The output current and voltage from the PV cell counts on the amount of the illumination on the surface of the cell and the temperature [44]. Moreover, the temperature has a direct effect on the output voltage. For instance, higher temperature results to a decrease in the output voltage. Equation 2.3 and 2.2 illustrate the relationship between the output voltage and current from the cell.

$$I = I_g - I_o \left[ e^{\left( \frac{qV}{kT} \right)} - 1 \right], \quad (2.2)$$

$$I = I_g - I_o \left[ e^{\left( \frac{V + IR_{sr}}{n k T_c / q} \right)} - 1 \right] - \left( \frac{V + IR_{sr}}{R_{sh}} \right), \quad (2.3)$$

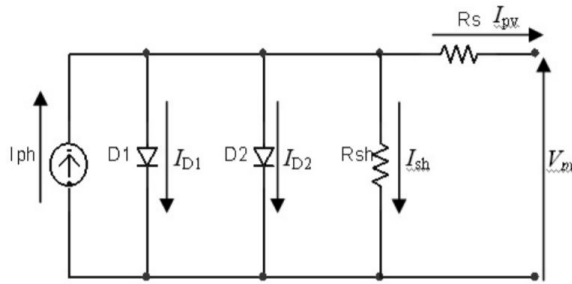


Figure 2.5: Equivalent circuit of PV cell [5].

where,  $I_g$  is the component of cell current due to photons;  $I_o$  is the saturation current;  $K$  is the Boltzmann constant which equal  $1.38 \cdot 10^{23} j/K$ ;  $T_c$  is the cell temperature;  $q$  is the electron charge ( $q = 1.6 \cdot 10^{19} C$ );  $V$  is the output voltage;  $R_{sh}$ , the shunt resistance and  $R_{sr}$ , the series resistance.

From equation 2.3, the temperature effects on the amount of the photo-current  $I_g$ . Moreover,  $I_g$  depends on the amount of solar irradiance falling on the PV cell. The relationship between the photo-current and solar irradiance ( $G$ ) and cell temperature ( $T_c$ ) can be given as:

$$I_g = I_{scR} \frac{G}{G_R} [1 + \alpha_T (T_c - T_{cR})], \quad (2.4)$$

The saturation current,  $I_o$  in equation 2.3 also known as the “dark-current” is a function of the cell temperature and the relationship is given by:

$$I_o = I_{oR} \left( \frac{T_c^3}{T_{cR}^3} \right) \exp \left[ \left( \frac{1}{T_{cR}} - \frac{1}{T_c} \right) \frac{q e_g}{nk} \right], \quad (2.5)$$

where,  $I_{oR}$  is the saturation current at the reference temperature,  $e_g$  is the band gap energy of the solar cell material and  $n$  is the diode ideal factor which is typically 1.3 for silicon solar cells [31].

The PV cell temperature,  $T_C$  ( $^{\circ}C$ ) can therefore be calculated as:

$$T_C = T_A + \left( \frac{NOCT - 20}{0.8} \right) G. \quad (2.6)$$

where,  $G$  is the solar irradiance,  $T_A$  is the ambient temperature and NOCT is the nominal operating cell temperature, which is the temperature that the PV cell will reach without any load connected. Equation 2.6 is expressed with air mass AM of 1.5 at  $20^\circ\text{C}$ ,  $G = 800 \text{ W/m}^2$  and the wind speed is less than  $1\text{m/S}$  [31].

### 2.4.2 PV module and array setup

A photovoltaic cell is a basic electrical component, which typically  $156 \text{ mm} \times 156 \text{ mm}$  dimension. Each cell produces about 0.5 volt when it is exposed to light. Moreover, the output amperage of the cell is proportional to its surface area, and counts on the light's intensity. PV cells can be connected together in series or parallel in order to have a PV module for voltage and power requirements. Common PV module contains between 54 and 72 cells [6]. 2.6 shows the configuration for PV cell, module and array.

PV cells within a module could be shaded by an external object or by clouds. Therefore, the shaded cell might become reverse-bias and consume power instead of produce it, which results to loss in the total output power. Furthermore, the PV cell could cause potential failure for the whole module, because the thermal stress on the other cells of the module. Sometimes, the extreme shading may generate reverse bias voltage that exceeds the breakdown voltage of the cell and damage the cell. Thus, PV cells can be connected in parallel to bypass diodes, which allow current to flow

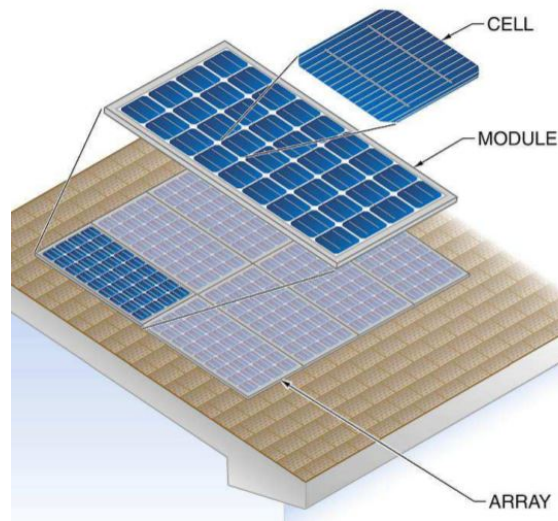


Figure 2.6: PV cell configuration from solar cell to solar array [6].

through the PV module. Without bypass diode, output power reduction can be up to 91.9%. It is sufficient to connect one bypass diode for each 15-20 PV cells. Moreover, bypass diode dose not cause any power losses since the current does not flow through it during the normal operation conditions. PV module has multiple cells that are connected in series and parallel as same as PV array that has multiple modules are connected in series and parallel [7]. PV modules are mainly connected in series in order to build voltage, while PV modules are connected in parallel in order to build current as shown in Fig. 2.7.

The PV array is static object, which can be mounted at a particular place in order to absorb the sunlight and then convert it to electricity. PV array received the maximum amount of irradiance when the sun is perpendicular to the array. However, the sun is changing its position to the earth during the daytime and the different

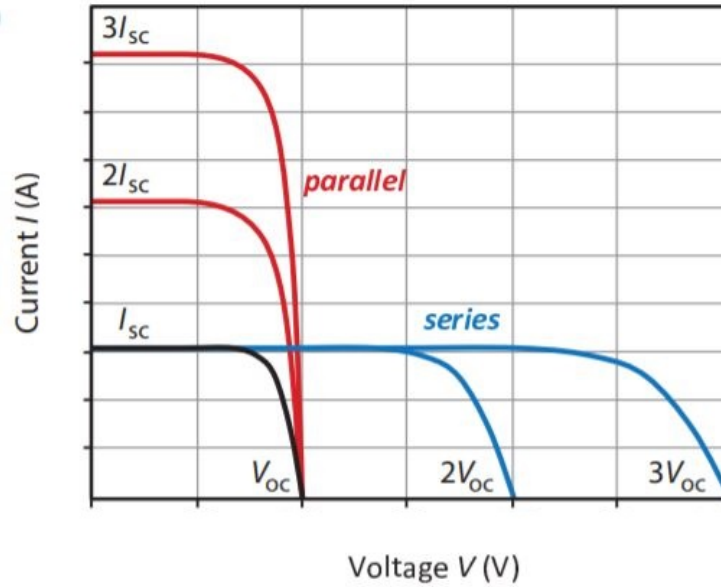


Figure 2.7: IV curve of PVs arrays with different configurations [7].

seasons. Therefore, it is impossible to have an orientation where the PV array will receive the maximum amount of irradiance. The position of the sun can be expressed by the solar azimuth and solar altitude. Solar azimuth represents the angle along the horizon, while the solar altitude represents the angle of the sun relative to the horizon of the earth where the north corresponds to angle of zero degree and increases in clockwise direction [7]. Solar altitude and solar azimuth change in term of time and day of the year for particular place. Moreover, solar constant represents the average rate of the radiant energy that is received from the sun on earth. For any day of the year, solar constant can be expressed as following:

$$I_{solar} = I_o \left[ 1 + 0.034 \left( \frac{360n}{365.25} \right) \right]. \quad (2.7)$$

Where  $I_{solar}$  the solar constant,  $n$  the desirable day of the year with January 1st being 1 [EquSolarConst]. The efficiency of the PV module is the ratio of the output electrical power to the solar irradiance input over the area of the cell [10], which can be expressed as:

$$\eta = \frac{P_m}{E * A}, \quad (2.8)$$

Where  $P_m$  the maximum power,  $E$  the solar irradiance ( $W/m^2$ ) and  $A$  the area of the PV module.

### 2.4.3 MPPT

Solar panels have a nonlinear voltage-current characteristics with certain maximum power point MPP, which counts on several factors such as temperature, irradiation and humidity. The maximum output power tracking is an electronic system that change the electrical point of the modules to generate the maximum output power. The maximum output power from the PV array counts on the electrical properties and conditions at the point of installation, while the operating point depends on the connected load [8]. PV panels always produce the maximum output power when operated at the knee of I-V curve as shown in fig 2.5.

There are several algorithms that can be used to calculate the maximum power point of the PV panels. Perturb and observe, incremental conductance and fuzzy logic

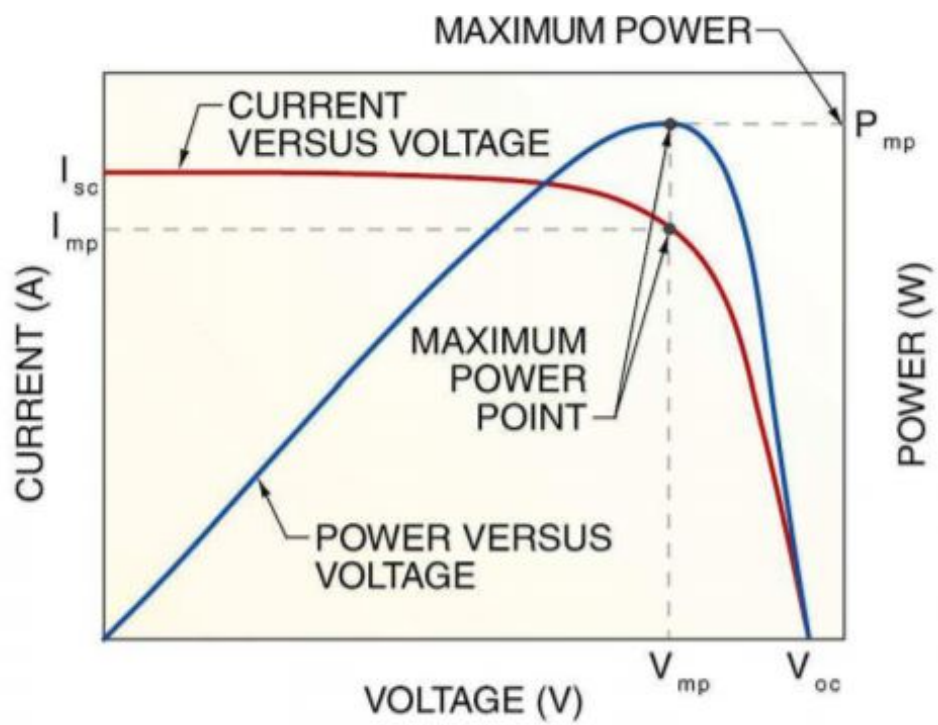


Figure 2.8: Solar Cell I-V Characteristic Curve [8].

are the most widely used algorithms. Perturb and observe algorithm is commonly used for MPPT due to the simplicity of the implementation process. Furthermore, incremental conductance algorithm needs more complicated computation inside the controller, which results in better track of changing conditions compared to the other algorithms [32].

#### **2.4.4 Converters and electric machines**

Power electronic converters mainly use for controlling the flow of the electric energy between two systems or subsystems [33]. It consists of solid states electronics such as diodes, thyristors and transistors that are used to control and convert the electric power from one form to another form such as DC to AC or AC to DC. In addition, it can be used to connect sources with loads, whose electric requirements are different from the source's output [34]. Electric machines are used to convert the energy from one form to another form such as mechanical energy to electric energy and vice versa. While motors convert the electric energy to mechanical energy, generators convert the mechanical energy to electric energy [35].

DC/DC converters are used for transforming DC source voltage from level to another level either high or low. Furthermore, switching converters regulate the current flow from input to the load. Linear converters preserves continuous current flow from the input to the load. Pulse with modulates converters (PWM) has high

efficiency, constant frequency, commercial availability and high conversion ratio [36]. The four main DC/DC topologies are boost, buck, buck-boost and Cuk converters [32]. A simple circuit implementation in PSCAD illustrates the variation of the output voltage with respect to duty cycle.

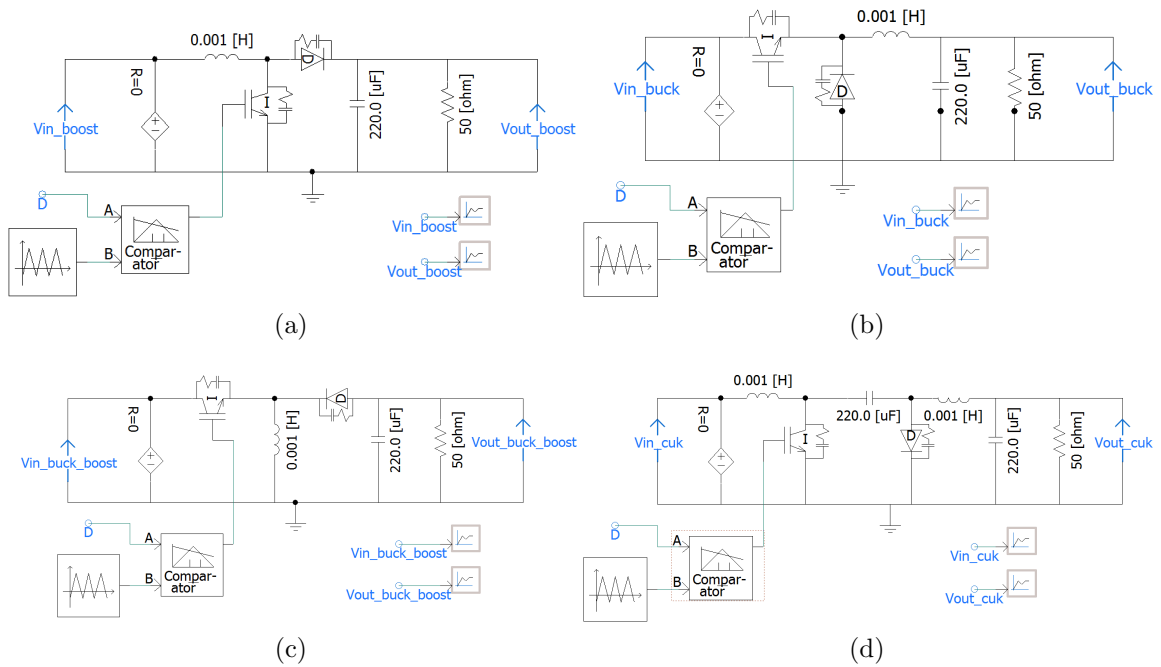


Figure 2.9: Circuit implementation in PSCAD for DC/DC converter (a) buck, (b) boost, (c) buck-boost and (d) Cuk [9].

AC/DC converters are mainly used to convert the electric power from AC to DC form, which known as rectifiers. DC/AC converters are used to convert DC to AC form, which known as inverters. AC/DC converters are used to supply DC power to the electronic devices such as computers, screen and battery charge controller. Rectifiers can be classified into controlled and uncontrolled rectifiers. While the output

of controlled rectifiers counts on the input and the external control system, the output of the uncontrolled rectifiers solely counts on the input [10]. The uncontrolled rectifiers are made of diode and can be classified into full bridge and half bridge diode rectifiers for one phase and three phase. Single phase full wave rectifiers consist of two diodes with transformer with center tap secondary side or four diodes without the transformer [37]. Half wave rectifiers only produce half output electric cycle, which requires less power electronics devices than the full wave rectifiers need. The correlation between the DC and the AC voltages of full-wave rectifier and half wave rectifier is expressed as:

$$V_{dc} = \frac{1}{2\pi} \int_0^\pi V_m \sin \omega t d(\omega t) = \frac{V_m}{\pi} = 0.318V_m \quad \text{for half bridge,} \quad (2.9)$$

$$V_{dc} = \frac{1}{\pi} \int_0^\pi V_m \sin \omega t d(\omega t) = \frac{2V_m}{\pi} = 0.636V_m, \quad \text{for full bridge.} \quad (2.10)$$

Where the input supply voltage is given as  $(V_m \sin \omega t)$  and  $V_{dc}$  the average load voltage [37].

## 2.5 Wind turbine

### 2.5.1 Wind turbine characteristics

Wind turbines consists of several parts that are employed to control the shaft speed, electromagnetic conversion, and extract the power from the wind. Firstly, wind turbine use blades to extract the power from the wind and then the low speed shaft will rotate. Secondly, a gear-train is employed to control the speed of the shaft for different conditions. For instance, step up the speed of shaft from the slowly spinning rotor to the higher speeds needed in order to drive the generator. Finally, for the conversion of the electromechanical energy, an electric generator is used for this purpose [17]. Power electronic converters may be used in order to regulate and control the output power of the turbine. Yaw system is used to rotate the nacelle in order to make the blades facing the wind direction. The main components of the wind turbine are illustrated in Fig 2.10.

Other components of the wind turbine are wind van and several sensors such as anemometer and current sensors. The wind van mainly measures the direction of the wind and then send a signal to yaw system. The sensors measure the speed of the wind for protection and maximum efficiency. In addition, other sensors are used to measure the voltage and current of the generator. Wind turbines are classified into four main types: fixed-speed, partial variable speed wind turbine with variable rotor resistance, variable speed wind turbine with partial-scale power converter and

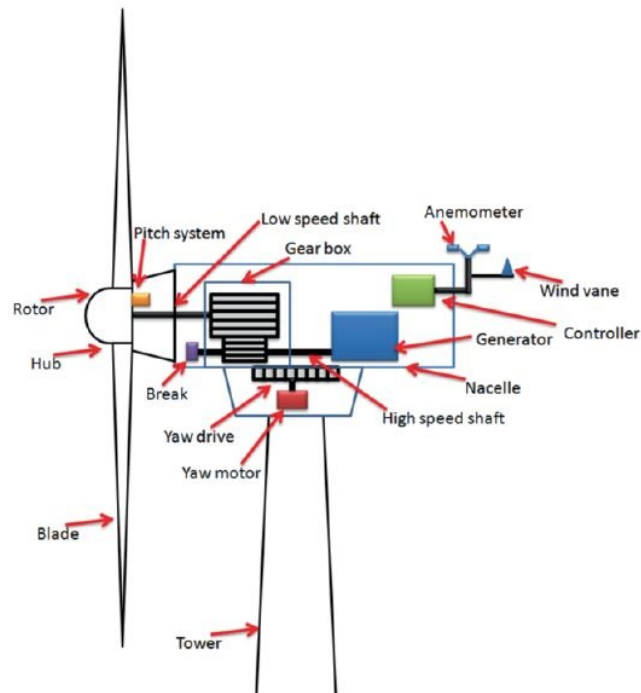


Figure 2.10: The components of the wind turbine [10].

variable speed wind turbine with full-scale power converter [65]. Fig2.11 shows the schematic of the fixed-speed turbine and the partial variable speed wind turbine with variable rotor resistance respectively, while fig2.12 shows the variable speed wind turbine with partial-scale power converter and the variable speed wind turbine with full-scale power converter [18].

Fixed-speed wind turbines are the most basic type. Which, operates with little variation in the speed of the rotor turbine. In addition, in this type of turbine, the generator is connected directly with the grid through a transformer. The second type is partial variable speed wind turbine with variable rotor resistance uses a wound rotor induction generator and is directly connected with the grid. Moreover, the winding of

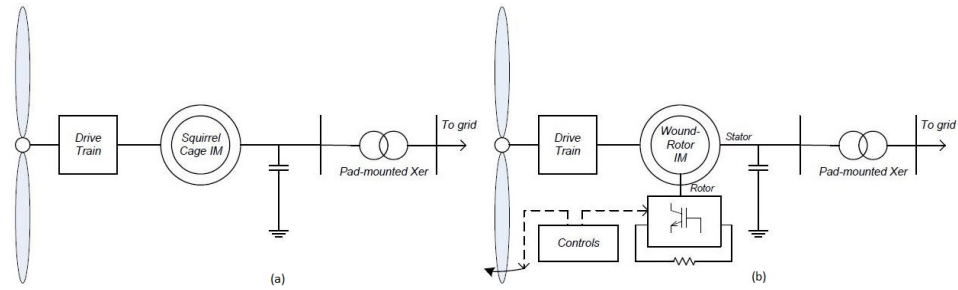


Figure 2.11: (a) Fixed-speed wind turbine, (b) partial variable speed wind turbine with variable rotor resistance [11].

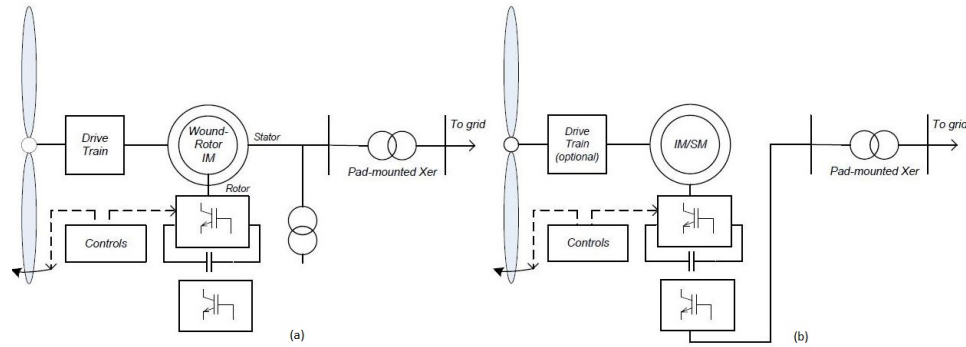


Figure 2.12: (a) Fixed-speed wind turbine, (b) partial variable speed wind turbine with variable rotor resistance [11].

the rotor is connected with controlled resistance in series in order to regulate the rotor resistance and control the output power. Variable speed wind turbine with partial-scale power converter, which known as doubly-fed induction generator wind turbines use AC/DC/AC converter inside the rotor to slide the power and to control the rotor frequency which results to control the rotor speed. Finally, variable speed wind turbine with full-scale power converter uses the permanent magnet generator (PMSG) with full scale power converter to connect with the grid [11]. In this model, the variable speed wind turbine with full-scale power converter uses (PMSG) to connect the

turbine with grid will be used. The generator is the main electrical component in the turbine. Synchronous generators (SG) are widely used in variable-speed wind energy conversion systems due to its large flexibility that meet the technical requirements in the wind energy systems. Moreover, it can be designed to have a large number of poles and operate at the same speed of the turbine blade. The wind energy system of the SG is controlled by full capacity converters due to the variable speed operation. The conventional two level back to back power converter is the most used converter for wind turbines. Using converter-based systems will allow independent real and reactive power control. Furthermore, the range of the converter is mainly between 1.5 to 3 MW. 2.13 shows the two main two level back to back converter [12].

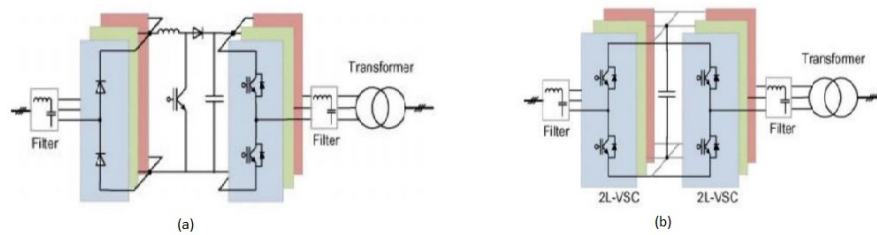


Figure 2.13: (a) Two level back to back converters with passive rectifier, (b) Two-level back-to-back converters with active rectifier [12].

The rated speed of the SG depends on number of poles and the rated stator frequency. 2.15 shows the construction of the variable speed SG wind energy system.

Generally, wind turbines operate from minimum speed, which known as cut-in speed, and then reach to maximum speed, which is the rated speed. The cut-in speed is the minimum speed that the turbine start generate the power. It is typically

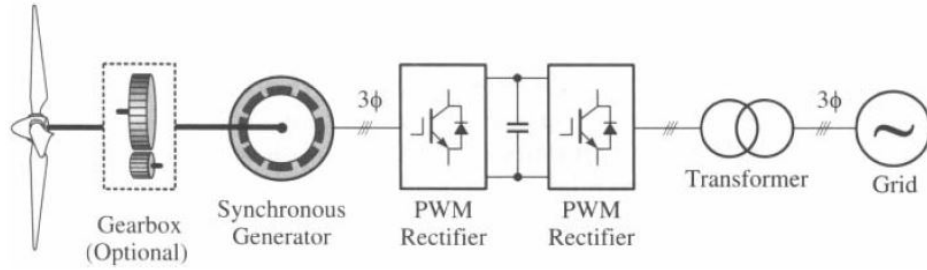


Figure 2.14: Block diagram of variable-speed SG wind energy system [13].

between 3.13 and 4.47 m/sec for most of the turbines. Therefore, the speed of turbine will increase until reach to the rated speed. Between the cut-in speed and rated speed of the turbine, maximum power point tracking will be operated in order to increase the power. The wind turbine will generate the designated power after the speed reach to the rated speed. To protect the parts of the turbine from the mechanical damage, wind turbine will be shut down at certain speed, which is usually between 22 and 45 m/sec. In addition, when the speed drops back to the rated speed, the wind turbine will operate again [13].

The power generated by a wind turbine could be expressed by the following equation:

$$P = \frac{1}{2} \rho_a C_P A_S V^3, \quad (2.11)$$

where  $\rho_a$  the air density in  $\text{kg/m}^3$ ,  $C_P$  the power coefficient,  $A_S$  the swept area of the wind turbine rotor in  $\text{m}^2$  and  $V$  the wind velocity in m/S. The swept area of

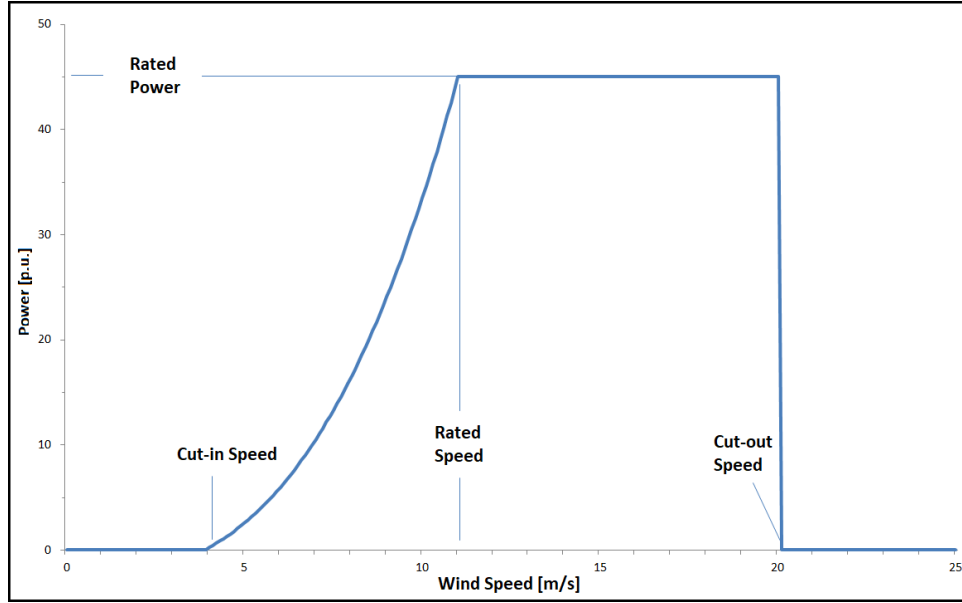


Figure 2.15: Wind power VS wind speed curve [13].

the rotor  $A_S$  can be further:

$$A_S = \frac{\pi}{4} D^2 = \frac{\pi}{r^2}, \quad (2.12)$$

The rotor power coefficient  $C_P$  can be expressed as following:

$$C_p = \frac{P_{rotor}}{P_{wind}}, \quad (2.13)$$

According to [13], the maximum power that can be extracted from wind can be calculated as:

$$P = \frac{16}{27} \frac{\rho_a}{2} V^3 A_S, \quad (2.14)$$

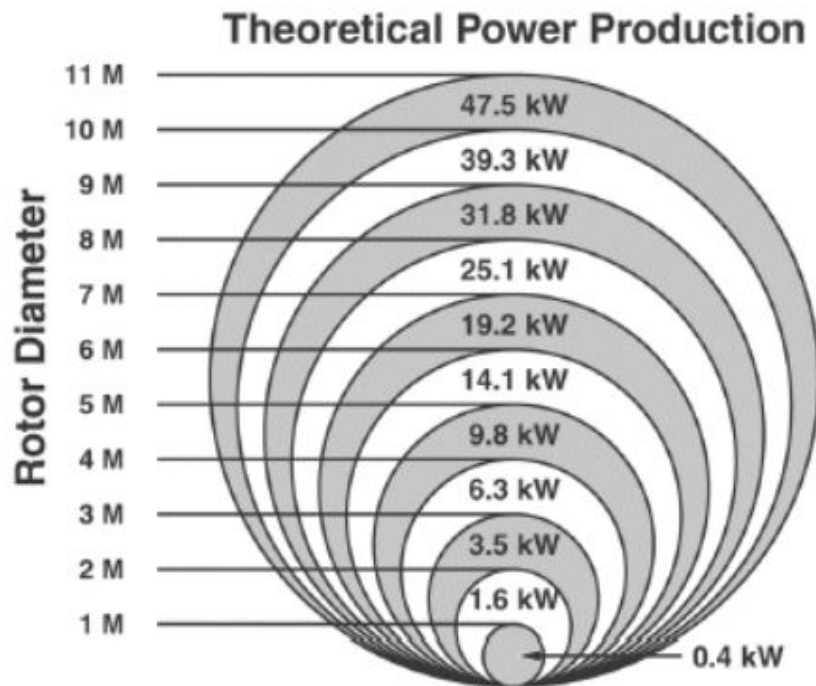


Figure 2.16: An example of theoretical power production against rotor's diameter change for small wind turbines at wind speed 10 m/s [14].

The relationship between the rotor's diameter and the generated power is significantly important. The increase in the rotor's diameter will lead to increases in swept area by the wind turbine, and hence, the amount of electricity that the turbine can generate. Figure 2.16 illustrates the changes in theoretical output power against the changes in rotor's diameter [13].

Another important factor related to the power of wind turbines is the tip speed ratio TSR, which is the ratio of the rotor tip's speed to the the free stream wind speed. Therefore, a high TSR is desirable, because it results in a high rotational speed of the shaft increases the efficiency of the electrical generator. Generally, slow

running blades operates with tip speed ratio between 1 to 4, and fast running blades operates with tip speed between 5 to 7. On the other hand, high TSR leads to noise, strong vibration especially for two and one blade rotors [12]. TSR can be calculates as following equation:

$$\lambda = \frac{v}{V} = \frac{\omega r}{V_{wind}}, \quad (2.15)$$

Where the rotor tip speed in [m/sec],  $V$  the wind speed in [m/sec],  $r$  the rotor radius in [m] and  $\omega$  the angular velocity in [rad/sec]. An important topology to improve the power coefficient  $CP$  is the blade pitch control. Unlike the wind speed, the pitch angle can be controlled in order to improve the performance of the wind turbine and extract the maximum available mechanical power regardless the wind speed. At constant speed ratio,  $C_p$  increases when the pitch angle decrease [23].

The mechanical torque is dependent on the wind speed, which can be expressed as :

$$T_m = \frac{P}{\omega}, \quad (2.16)$$

Furthermore, any wind turbine can not convert more than 0.593 of the kinetic energy of the wind into mechanical energy that turns a rotor and it is called the power coefficient  $C_p$ . In addition, It is known as Betz law who concluded the law. Therefore, the power coefficient can be (0.593 or less) [23].

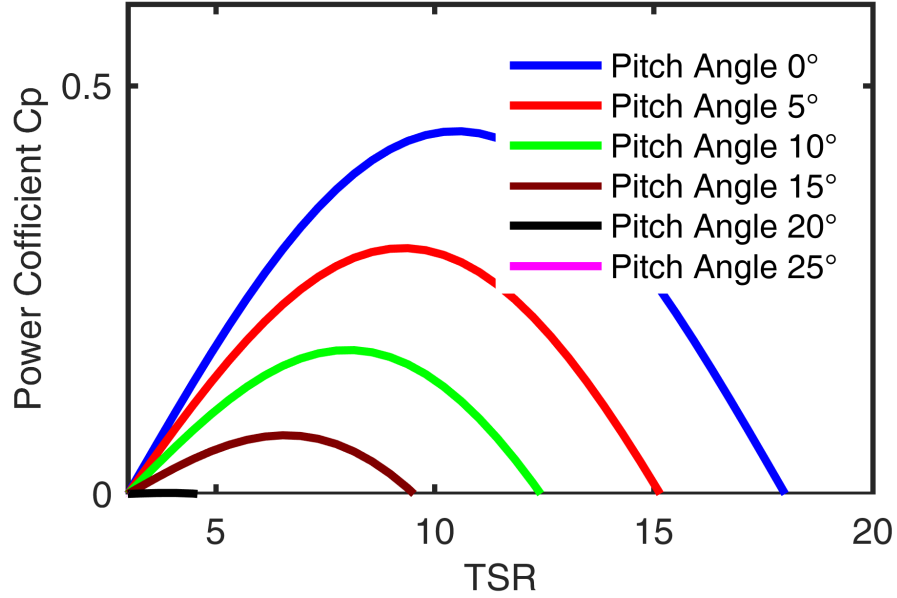


Figure 2.17: Power coefficient  $C_p$  as a function of TSR  $\lambda$  and pitch angle in degrees.

## 2.5.2 Wind turbine controllers

Wind speeds varies depends on the environment and the time. Thus, the rotating speed of the wind generator is not constant, which is different from the electrical synchronous speed of the grid. Therefore, the electrical base frequency of the wind generator should be set to a value with respect to the rates mechanical speed of the wind turbine [24]. Equation 2.17 and 2.18 illustrate the value for the electrical base speed of the synchronous machine.

$$f_{base} = \frac{P}{2} \cdot \frac{RPM_{TUR}}{60}, \quad (2.17)$$

$$\omega_B = 2\pi f = \pi.P.\frac{RPM}{60}, \quad (2.18)$$

Wind turbines contain control system that is used to increase the output efficiency and decrease the loads on the structure. Control system consists of several computers to continuously monitor the direction and speed of the wind. In addition, it collects and analyze the data that are receive it from sensors. Furthermore, yaw system actively adjust the angle of attack based on the direction and the measurements of the wind. Therefore, the control system mainly controls the yaw system, the blade pitch system and the generator. To collect the data of the wind such as direction and speed, there are several sensors that can be used. For instance, a cup anemometer which measures the wind speed and send it to the central controller. Another type of sensors that can be used is ultrasonic anemometer. It sends high frequency waves between the four poles and then it measures the phase shifting in the received signals. In addition, the type of generators that can be used for the wind turbine are doubly fed induction generator (DFIG), squirrel cage induction generator (SCIG), wound rotor induction generator (WRIG), permanent magnet synchronous generator (PMSG) and finally electrically excited synchronous generator (EESG). The most using generators are DFIG and SCIG generators [24].

### 2.5.3 Permanent magnet synchronous generator model

Permanent magnet synchronous generator is the most important part in the wind power generation system, which transfer the mechanical power into electrical power and then connect with grid. The PMSG will generate the power and then it will be transferred to the power converters, which control the power before send it to the grid. The converters are required because the PMSG generates a variable frequency voltage that need to match the constant grid voltage [38]. The state space relationship between the terminal voltage of the PMSG and the currents and the phase flux linkages in abc reference can be expressed as following:

$$\begin{bmatrix} v_{as} \\ v_{bs} \\ v_{cs} \end{bmatrix} = \begin{bmatrix} R_s & 0 & 0 \\ 0 & R_s & 0 \\ 0 & 0 & R_s \end{bmatrix} \begin{bmatrix} i_{as} \\ i_{bs} \\ i_{cs} \end{bmatrix} + \frac{d}{dt} \begin{bmatrix} \lambda_{as} \\ \lambda_{bs} \\ \lambda_{cs} \end{bmatrix} \quad (2.19)$$

Where,  $v_{as}$ ,  $v_{bs}$  and  $v_{cs}$  the instantaneous three phase stator voltages in abc reference,  $i_{as}$ ,  $i_{bs}$  and  $i_{cs}$  the instantaneous three phase stator current in the same reference, and  $\lambda_{as}$ ,  $\lambda_{bs}$  and  $\lambda_{cs}$  the instantaneous flux linkage, which can be expressed in the following equation:

$$\begin{bmatrix} \lambda_{as} \\ \lambda_{bs} \\ \lambda_{cs} \end{bmatrix} = \begin{bmatrix} L_{aa} & L_{ab} & L_{ac} \\ L_{ba} & L_{bb} & L_{bc} \\ L_{ca} & L_{cb} & L_{cc} \end{bmatrix} \begin{bmatrix} i_{as} \\ i_{bs} \\ i_{cs} \end{bmatrix} + \begin{bmatrix} \lambda_r \cos(\theta_r) \\ \lambda_r \cos(\theta_r - \frac{2\pi}{3}) \\ \lambda_r \cos(\theta_r + \frac{2\pi}{3}) \end{bmatrix} \quad (2.20)$$

Where,  $L_{aa}$ ,  $L_{bb}$  and  $L_{cc}$  the self inductance of three phases ,  $L_{ab}$ ,  $L_{ac}$ ,  $L_{ba}$ ,  $L_{bc}$ ,

$L_{ca}$  and  $L_{ca}$  the mutual inductance between phases,  $\lambda_r$  the rotor flux linkage and  $\theta_r$  function of both self and mutual inductance [38]. On the other hand, the voltages of the PMSG in dq reference can be expressed as following:

$$v_{ds} = R_s i_{ds} + L_d \frac{di_{ds}}{dt} - \omega_e L_{qs} i_{qs}, \quad (2.21)$$

$$v_{qs} = R_s i_{qs} + L_d \frac{di_{qs}}{dt} - \omega_e L_{ds} i_{ds} + \omega_e \lambda_r, \quad (2.22)$$

Where,  $v_{ds}$  and  $v_{qs}$  the instantaneous stator voltages in dq reference,  $i_{ds}$  and  $i_{qs}$  the instantaneous stator current in dq reference,  $L_d$  and  $L_q$  the inductance in dq reference and  $\omega_e$  and  $\lambda_r$  the electrical angular speed and flux linkage respectively [38]. The cut-in speed is determined by the parameters of the turbine as well as the cogging torque of the motor. It must be small as much as possible to increase the efficiency of the turbine. In addition, cogging torque affected by several design factors such as air gap length, magnet performance, slot opening and pole pitch of the magnet [12]. The electromagnetic torque of the generator can obtained as:

$$T_e = \frac{3}{2} P (\lambda_r i_{qs} - (L_d - L_q) i_{ds} i_{qs}), \quad (2.23)$$

Where P the number of pole pairs,  $\lambda_r$  rotor flux-linkage (Wb),  $L_d$  and  $L_q$  are dq-axis stator self inductance respectively and  $i_{ds}$  and  $i_{qs}$  are dq-axis stator currents respectively.

The d-axis stator current  $i_{ds}$  could be controlled to be zero in order to have a linear relationship between  $T_e$  and the stator current at constant rotor flux linkage  $\lambda_r$ . Therefore, 2.23 can be simplified as:

$$T_e = \frac{3}{2}P(\lambda_r i_{qs}) = \frac{3}{2}P(\lambda_r i_s), \quad (2.24)$$

The magnitude of the stator voltage could be expressed as:

$$V_s = \sqrt{(v_{ds})^2 + (v_{qs})^2} = \sqrt{(\omega_r L_q i_{qs})^2 + (\omega_r \lambda_r)^2}, \quad (2.25)$$

The stator power factor angle is expressed as:

$$\phi_s = \theta_v - \theta_i, \quad (2.26)$$

Where  $\theta_v$  and  $\theta_i$  are the angles of the stator voltage and current vectors respectively, given by:

$$\theta_v = \tan^{-1}\left(\frac{v_{qs}}{v_{ds}}\right), \quad (2.27)$$

$$\theta_i = \tan^{-1}\left(\frac{i_{qs}}{i_{ds}}\right), \quad (2.28)$$

## 2.5.4 PSCAD model

Wind power is an important resource of energy that could be used to increase the capacity and the reliability of the grid. There are several types of wind turbines used for this industry. One of these types is the full converter wind turbine using a permanent magnet synchronous generator. Many advantages can be achieved by using this technology. For instance, allowing the turbine to operate over a wide range of wind speeds, which results in improved power extraction from the grid. Moreover, improving the fault response of the system, which increases the reliability of the grid [39].

Integration of the wind turbines with the grid requires steady state studies and dynamic transient studies of the turbines along with its collector system in order to simulate the impact of the dynamic events on the power system such as loss of generation, loss of wind, loss of generation, short circuit voltage and loss of lines. Power electronics has a significant effect on the system since it controls the output power from the generator. The interface between the generator and the grid is AC-DC-AC conversion system. The AC-DC converter consists of diode bridge rectifier and a buck-boost converter in order to control the DC link voltage. Furthermore, the DC-AC conversion is using a current controlled inverter, which regulates the reactive and real power of the system. Full converter wind turbine consists of different subsystems, which are electrical and mechanical subsystems. It consists of aerodynamic model for

rotor, reference power calculations, pitch controller, power electronics subsystem and PMSG model. In this model, wind turbines rated of 2 MW from Vestas company will be used. In addition, the full technical data is as appendix at the end of the report. Power system simulation tools PSCAD/EMTDC will be used to simulation studies. The aerodynamic torque (see also equation 2.23 can then be calculated as:

$$T_{rotor} = \frac{P_{rotor}}{\omega_{rotor}} = \frac{\frac{1}{2} \cdot \rho \cdot C_p \cdot \pi R_{rotor}^2 \cdot V_{wind}^3}{\omega_{rotor}}, \quad (2.29)$$

Where  $C_p$  the rotor power coefficient and can be expressed as following:

$$C_p = \frac{P_{rotor}}{P_{wind}}, \quad (2.30)$$

The TSR  $\lambda$  and the user-defined blade pitch angle  $\beta$  are used to calculate the rotor power coefficient  $C_p$  as following:

$$C_p = 0.5(\lambda - 0.022\beta^2 - 5.6)e^{-0.17\lambda}, \quad (2.31)$$

Since the wind turbine in this model will be installed close to the sea level, the air density  $\rho$  is 1.23 kg/m. Therefore, from (3.3), the power of the turbine can be calculated as :

$$P = 0.5 * 1.23 * 9852 * 0.5 * 12^3 = 5.192MW, \quad (2.32)$$

From equation 2.33, the theoretical output power is larger than rated power of the turbine, because the Betz law, which means that wind turbines can not be better than 0.59 efficient. Therefore, the rated output power would be:

$$P = 5.192 * 0.59 = 3.06MW, \quad (2.33)$$

The mechanical torque of the generator is dependent on the power and the wind speed (as explained in equation 2.16.  $T_m = 1450/3.06M = 2068.9$  N.m

Table 2.2: Generator data

Type	Permanent Magnet synchronous generator
Rate Power (MW)	2
Rate Apparent Power (MVA)	2.35
Rated Voltage (kV)	0.71
Rated Current (kA)	11.5 to 14
Rated Speed (rpm)	1450
Number of Poles	12
$X_d$	0

Table 2.3 illustrates the parameters of the turbine that is used in the module. In addition, the wind governor parameters is defined in Table 2.4.

Conductor rotor MVA	3 [MVA]
Machine rotor angular speed	3.14 [rad/sec]
Rotor Radius	46.2 [m]
Rotor Area	710 [m <sup>2</sup> ]
Air Density	1.225 [kg/m <sup>3</sup> ]
Gear Box Efficiency	1 [p.u]
Gear Ratio	1

Table 2.3: The wind turbine parameters.

The parameters of the synchronous generator component are shown in table 2.5.

Variable Pitch control	Enabled
Type of Generator	synchronous
Rated angular Frequency	3.1416 [m]
Machine rated Power	3.6 [MW]
Turbine Rated Power	3.0 [MVAR]

Table 2.4: The wind governor parameters.

Rated RMS Line-Neutral Voltage	0.69 [kV]
Rated RMS Line Current	1.45 [kA]
Base Angular Frequency	314.16 [rad/sec]
Inertia Constant	6.3 [s]
Mechanical Friction and Wind	0.02 [p.u.]
Neutral Series Resistance	20 [p.u.]
Neutral Series Reactance	0.0 [p.u.]

Table 2.5: The synchronous generator parameters.

Finally, the schematic of the model is shown in fig. 2.18

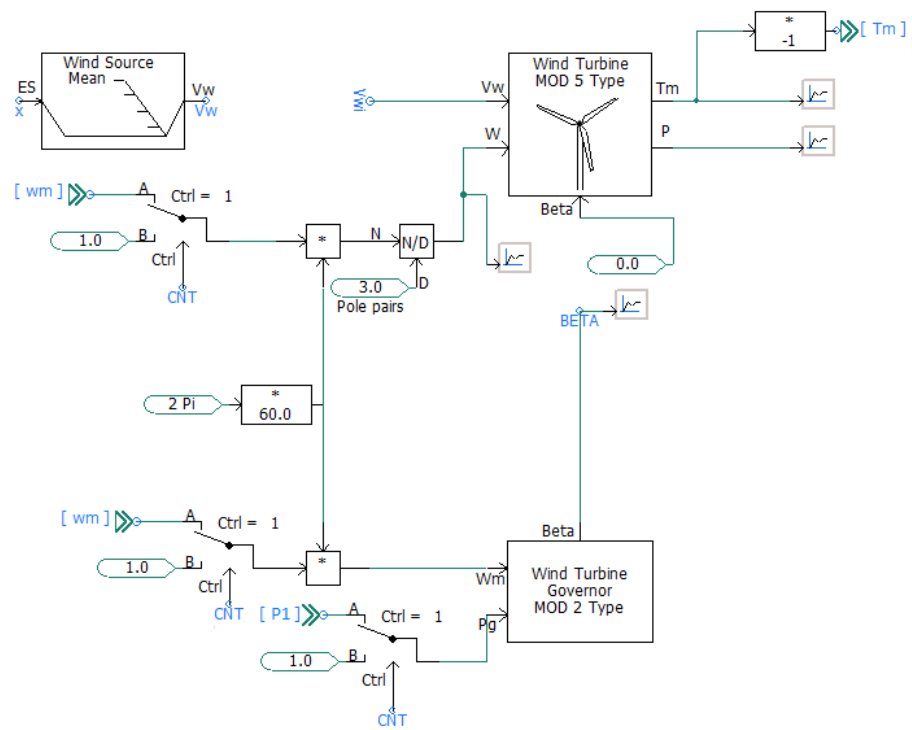


Figure 2.18: PS-CAD Model of a wind turbine generator.

# Chapter 3

## Simulation of PV, Wind Turbine, Water Desalination Plant and the Grid

This chapter explains the control and protection for integrating the PV, the wind turbines and water desalination plant with the grid. PV is divided into several parts and every part has separate DC/DC converters and two levels inverter in order to grid voltage control. The wind turbines also divided into several parts and each part has its own AC/DC converter and DC/AC inverter. The water desalination plant is expressed as constant speed pumps, which represent the water desalination process. The PV arrays, the wind turbines and constant speed pumps are connected to the electric grid with different operation modes.

### 3.1 Introduction

Renewable energy resources are expected to be essential proportion of the future smart grid. According to the institute for energy research [1], about 9.9% of the total

consumed energy In 2015 was from renewable resources. In addition, about 24.42 GW of PV was installed between 2010 and 2015. Several countries over the world use the renewable resources as a portion of their grid. For instance, Germany and China generate about 39.7 GW and 43.5 GW respectively from the PV in 2015 [1]. Thus, it is significant to study the effect of the integrating the wind turbines and PV with the grid. A substantial amount of literature exists on renewable resources integrated with the grid, and some of these literatures are on energy storage systems and maximum power point tracking techniques [5]. Some authors discuss the control of the voltage and frequency of the grid [30]. Total harmonic distortion of the injected current to the grid was explained [40, 41]. Other researches explained the typologies for DC-DC converter, PV inverters and AC-DC converters [42]. Each section of the PV systems has a PV array, DC-DC, transformer and DC-AC converter connected in parallel in order to connected the PV array with the grid as shown in Fig3.1.

The two level inverters could be cascaded with proper control to obtain a multilevel output voltage waveform. Moreover, each inverters connected with the grid through 2 winding transformer. For wind power system, it is divided to several sections and each section has wind blades, PMSG, AC-DC converter and DC-AC inverter as illustrated in fig3.2.

The conversion system consists of converter for rotor side, another converter for grid side and control system for the converters. Conversion topology accomplished

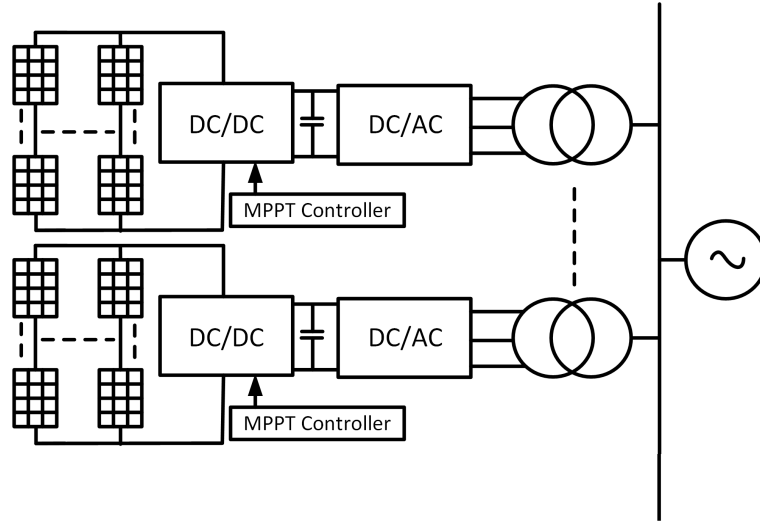


Figure 3.1: Schematic of grid tied PV system consists of multiple units connected in parallel with one transformer [9].

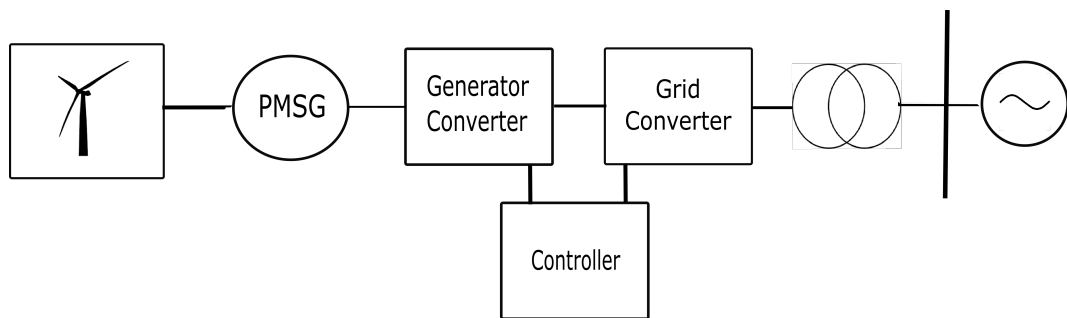


Figure 3.2: The schematic of grid tied wind turbine system including a wind turbine connected with one PMSG, converters and transformer.

by a diode-bridge rectifier and a buck-boost converter, which controls the DC link voltage. The DC-AC conversion is using a current-controlled inverter, which controls the real and reactive output power.

## 3.2 PV System

PV system has been divided into several section in order to meet the power conditioning electronics requirements [43]. Each sections include a buck converter connected with the PV array to maintain the output voltage at the maximum power point. When multiple strings are connected together, [44] suggests using the buck converter for maximum power point tracking. The buck converter is connected with two level central inverter via DC link capacitor.  $\Delta$ -Y transformer could be used to connect the PV with the grid. Fig3.3 shows the schematic of the one PV section in PSCAD.

Practical implementations may use a  $\Delta$ -Y transformer also [22].

### 3.2.1 PV array

Photovoltaic cell mainly converts the light energy into electricity. The intensity of the radiation on the cell controls the current, while the increase in the temperature of the cell results on reduce the voltage. The solar cell will have its maximum voltage when no load is connected with the cell, which known as open circuit voltage ( $V_{oc}$ ) and the solar cell current will be its minimum. On the other hand, when the solar

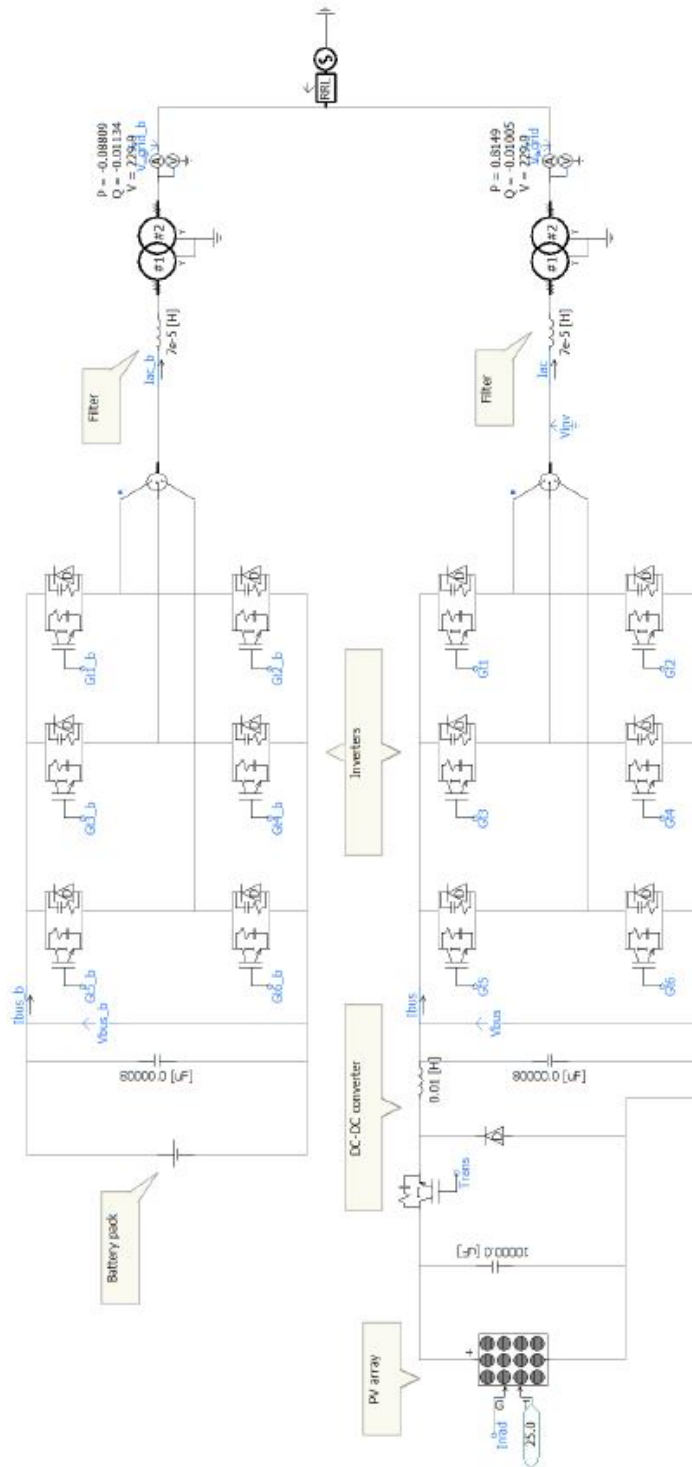


Figure 3.3: Schematic of PV unit in PSCAD showing the solar PV panel, 2-level inverter, DC-DC converter, transformer and grid based on [9].

cell is short circuited, the voltage will be its minimum and the current reaches its maximum, which known as short circuit current ( $I_{sc}$ ). Thus, solar cell will produce its maximum electric power at the knee of the I-V curve as shown in fig3.4, which known as MPP [9].

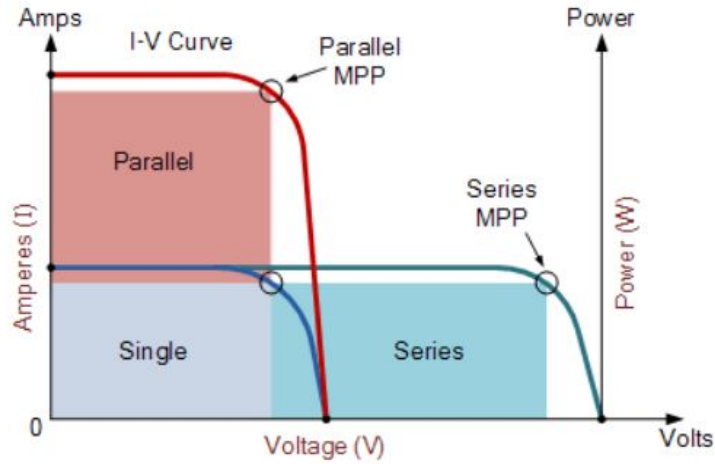


Figure 3.4: Solar panel I-V characteristics curve [9].

The relationship between voltage and current of the PV cell is expressed as:

$$I_{cell} = I_g - I_o \left[ e^{\left( \frac{q(v + I_{cell}R_{sr})}{nKT_c} \right)} - 1 \right] - \left( \frac{v + I_{cell}R_{sr}}{R_{sh}} \right), \quad (3.1)$$

where,  $I_g$ , the photo current generated;  $I_o$ , the saturation current;  $K$ , the Boltzmann constant;  $q$ , the electron charge;  $V$ , the output voltage;  $T_c$ , the cell temperature;  $R_{sh}$ , the shunt resistance and  $R_{sr}$ , the series resistance [42]. Open circuit voltage of the cell ( $V_{oc}$ ) typically varies from 23.3 to 44.2 V when tested under standard test conditions (STC) and depending on the material of cell. In this PV system, each

module consists of two strings connected in parallel with 40 cells connected in series per string in order to achieve  $V_{oc}$  of 43.7V and short circuit current of 9.12A per module under (STC). In addition, the PV array consists of 160 strings of PV module with 24 modules per strings in order to keep the DC voltage below 1kV. Table3.1 shows the PV cell and module specifications in the PV system.

Table 3.1: PV cell and module specifications

<b>Parameters</b>	<b>Value</b>
PV cell open circuit voltage $V_{oc}$ (V)	1.09
PV cell short circuit current $I_{sc}$ (A)	4.56
PV module open circuit voltage (V)	43.7
PV module short circuit current (A)	9.12
Maximum power (W)	260

### 3.2.2 MPPT

Maximum power point tracking MPPT is an electronic system that varies the the operating point of the PV module in order to deliver the maximum available power. The output power from the PV module depends on the environment conditions such as the temperature and irradiation. Therefore, MPPT is used in order to produce the maximum power from the PV module, which is at the knee of the I-V curve at every conditions [41]. In this model, the incremental conductance method will be used. Before the incremental conductance method determines the reference voltage ( $V_{mpt}$ ) based on MPP, the output voltage ( $V_{PV}$ ) and current ( $I_{PV}$ ) of the PV array is continuously measured and filtered as illustrated in fig3.5 . Therefore, the PI

controller is used to ensure that the ( $V_{PV}$ ) is equal to ( $V_{mppt}$ ) by changing the duty cycle of the DC-DC converter and compare it with a high frequency triangular signal generator in order to produce the IGBT gating pulse as shown in fig3.6.

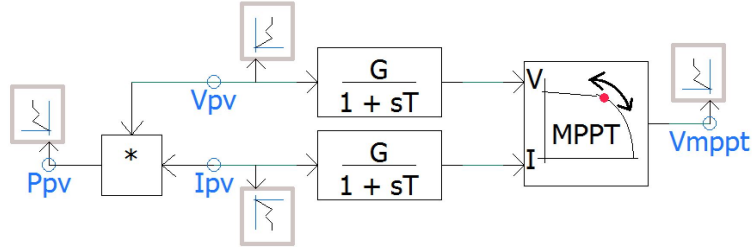


Figure 3.5: Schematic diagram for MPPT control in the PSCAD [9].

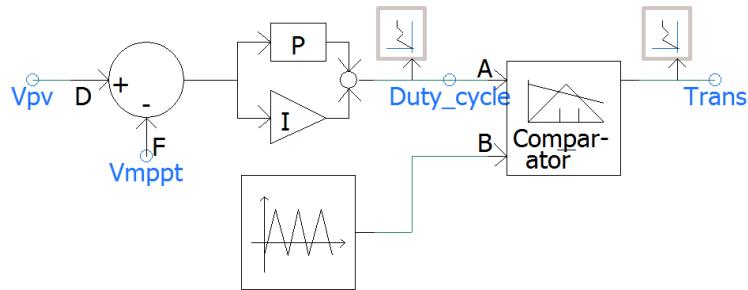


Figure 3.6: Control diagram for DC-DC converter in the PSCAD [9].

### 3.3 Wind turbine

Wind energy system has been divided into six separate sections, and each section produces 2 MW. Each section has mechanical and electrical components. The mechanical components extracts the power from the wind turbine and produce mechanical torque. The electrical components converts the mechanical torque to an

electrical torque and generate electric power. Permanent magnet synchronous generator PMSG is the interface between the mechanical and the electrical components [39]. The electrical consists of two converters for grid side and rotor side, converters control and measurements multi-meters. The mechanical system consists of the wind turbine and pitch angle controller. Fig3.7 illustrates the PSCAD module for one wind turbine of 2 MW, which includes the PMSG, converters with controller and transformer.

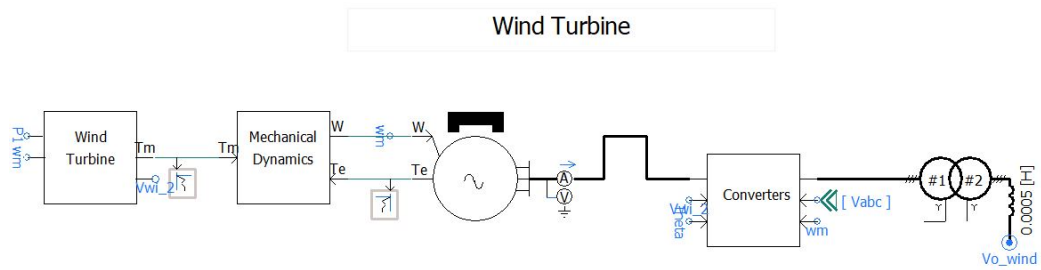


Figure 3.7: Schematic of 2MW wind turbine unit in PSCAD showing the turbine, mechanical dynamic block, PMSG, AC-DC converter, DC-AC converter and transformer.

The electrical generator is used in this model is a three-phase permanent magnet synchronous generator since it has a high efficiency with less maintenance. Also, it is used for different speed variation [38]. 3.2 illustrates the electrical specifications of the PMSG in PSCAD simulation.

Table 3.2: Electrical specification of the generator

Type	Permanent magnet synchronous generator
Rated power	2 MW
Rated apparent power	2.35 MVA (@pf=0.85)
Rated speed	1450 rpm
Frequency	145 Hz
Voltage	710 V
Number of poles	12

### 3.3.1 AC/DC/AC converters

The wind speed is variable and typically depends on the time of the day. AC-DC-AC conversion system must be used in order to regulate and connect the output power of the generator with the grid. Three system variables must be controlled in order to regulate the output power from the PMSG, which are the maximum output power that are produced by the turbine, the reactive power injected to the grid and the DC link voltage of the power converters [14]. The conversion system consists of rotor side converter and grid side inverter. While the rotor side converter controls the active power by controlling the current of the rotor circuit, the grid side converter controls the DC bus voltage and reactive power to the grid [11]. Fig3.8 illustrates the schematic diagram for the control system of the conversion system that are used in the model. In addition, using fully controllable rectifier permits variable speed operation, and maximum power point tracking for different wind speeds. Fig3.9 Fig3.13 illustrate the schematic diagram for the rectifier control and the PSCAD model for the same system respectively. Hysteresis current control is a PWM technique, which has implemented

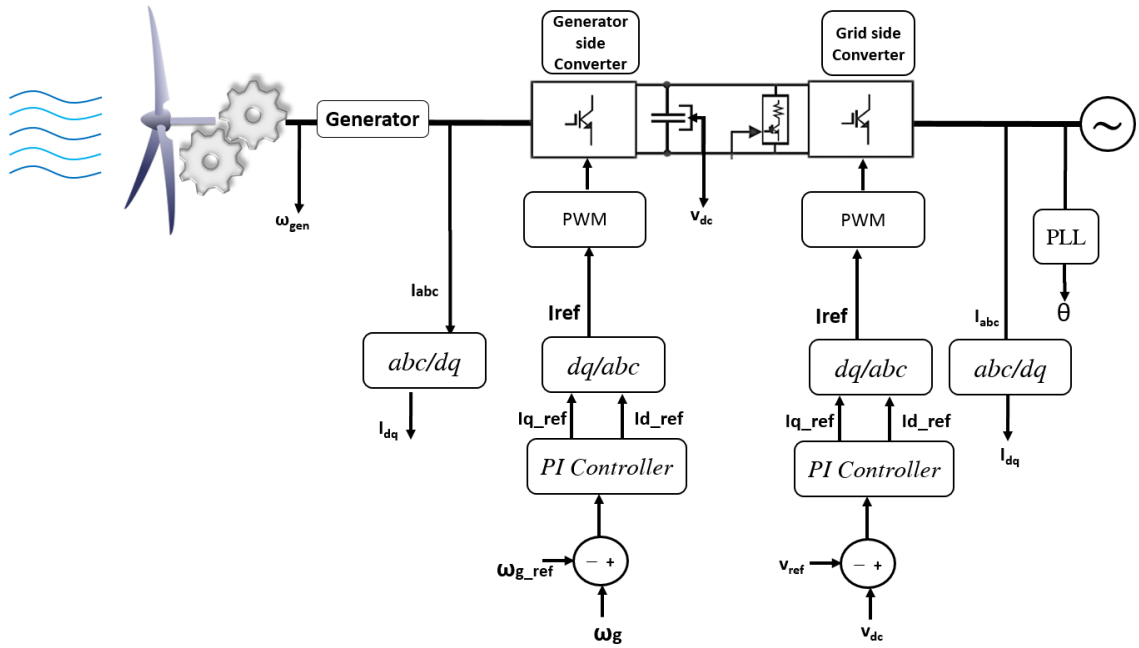


Figure 3.8: Schematic diagram for the control system of the conversion system.

in this control system of the converters for its simplicity and is used for high rating power system. It operates by comparing a current error such as the difference between the measure phase current and the demand current [45]. Furthermore, when the error exceeds the upper hysteresis band, the converter output is switched low and vice versa. Pulse width modulation PWM controller can be used in this system, which can get much less ripple in the controller currents. Fig3.13 shows PSCAD model for the same system.

As shown in figure3.11, the reference speed of the generator  $\omega_{ref}$  is calculated based on the pitch control topology, and then compare it with the measured generator speed. Thus, the error are sent to PI controller, which generate q-axis reference current  $i_{qref}$ .

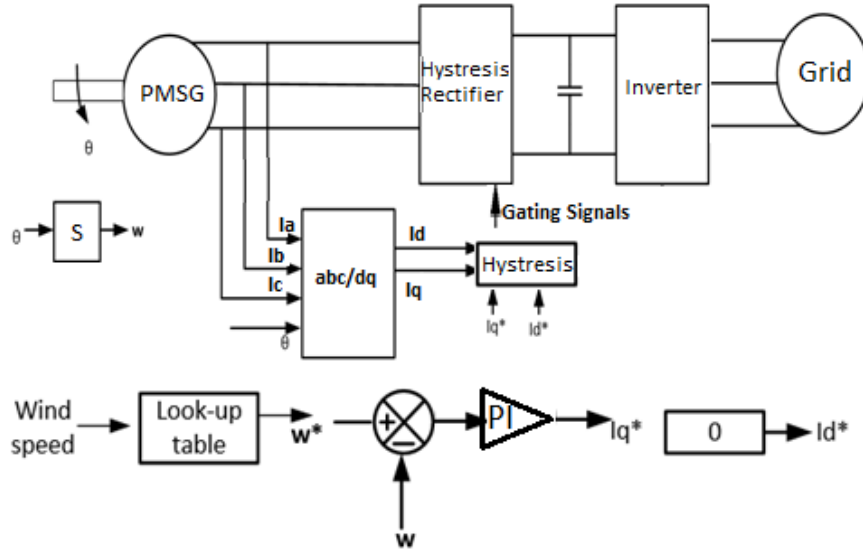


Figure 3.9: Schematic diagram for the rectifier control based on [15].

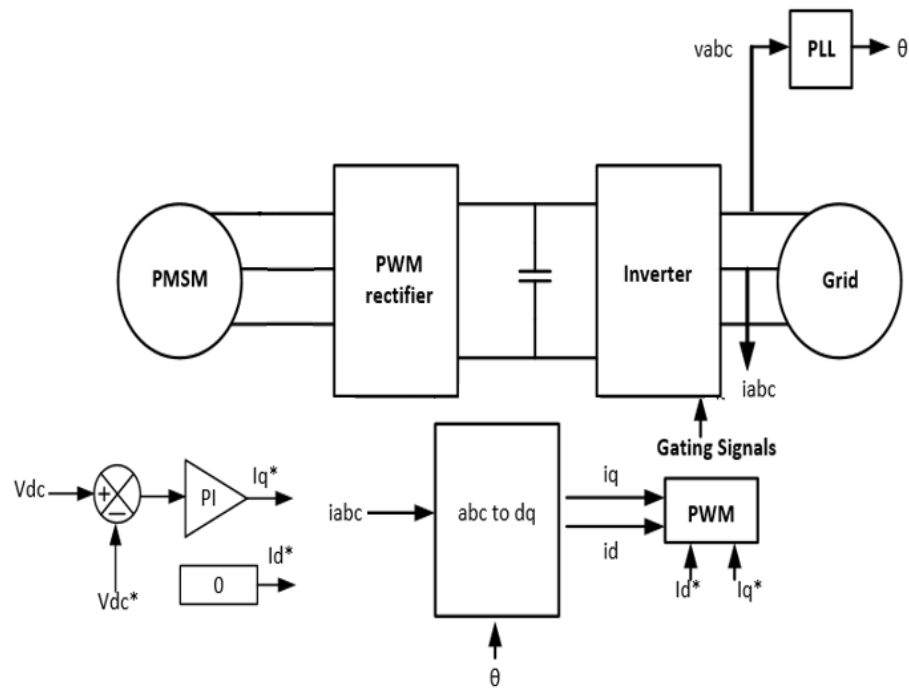


Figure 3.10: Schematic diagram for the inverter control based on [15].

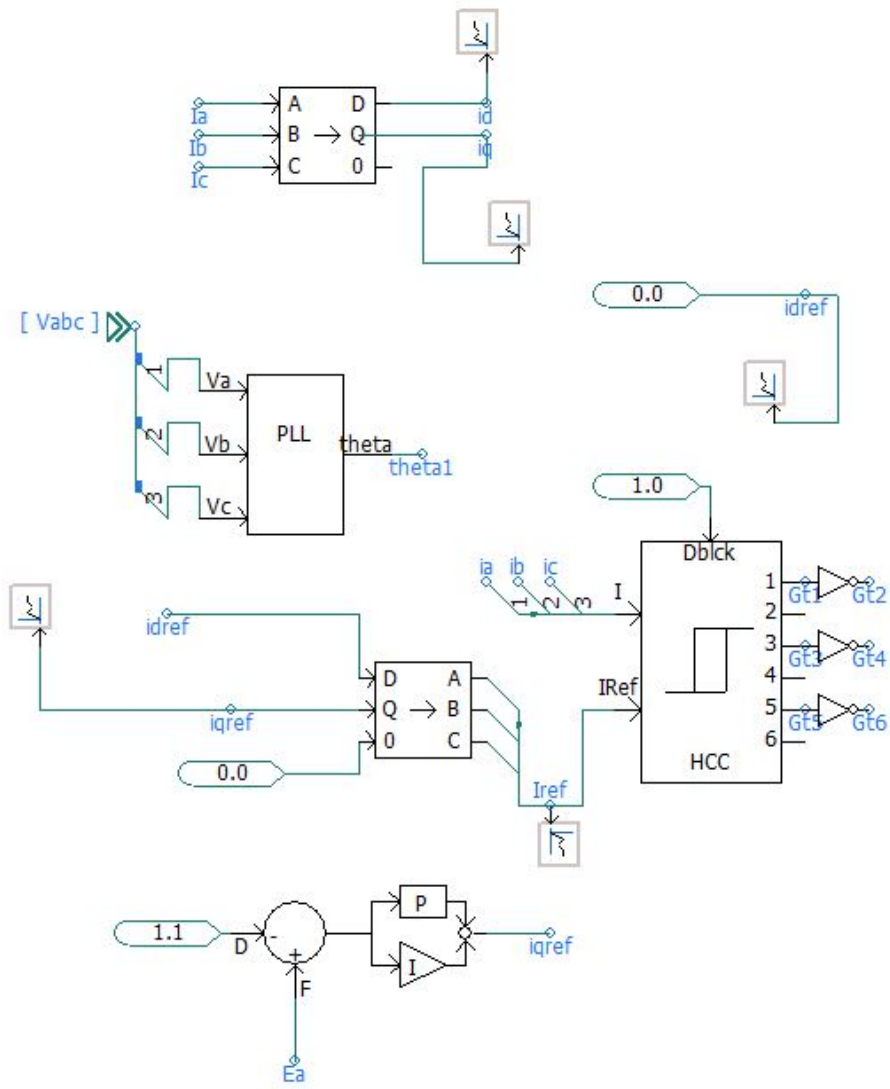


Figure 3.11: Power circuit diagram in PSCAD simulator shows the control system that are used for the converters.

The d-axis reference current of the stator  $i_{dref}$  is set to be zero in order to realize the zero  $d$ -axis control (ZDC) topology. Thus, the stator current is equal to its  $q$ -axis component  $i_{qs}$  as following:

$$i_s = \sqrt{i_{qs}^2 + i_{ds}^2} = i_{qs}, \quad (3.2)$$

Furthermore,  $i_{dref}$  and  $i_{qref}$  are transformed into abc stationary frame by using dq/abc block. The three measured currents  $i_a$ ,  $i_b$  and  $i_c$  can be adjusted by using PWM block, which adjust them according to their reference values. In addition, the three phase stator currents  $i_{as}$ ,  $i_{bs}$  and  $i_{cs}$  are transformed into dq-axis currents  $i_{ds}$  and  $i_{qs}$  respectively. The  $d$ axis current is set to be zero and the  $q$ axis current is controlled in order to control the electromagnetic torque  $T_e$  [25]. The measured grid voltages are sent to a phase locked loop (PLL) control to track the grid voltage vector and generate the angle of the grid voltage  $\theta$  for the voltage oriented control (VOC) as shown in fig3.12. Fig3.13 shows the circuit diagram for the rectifier, inverter and control system.

### 3.3.2 Phase locked loop

A phase locked loop (PLL) is a closed-loop system, which an internal oscillator is controlled to keep the time of some external periodical signal by using the feedback loop [27]. In addition, PLL techniques are used in many fields such as power electronics, communications and computers. Grid connected power converters match

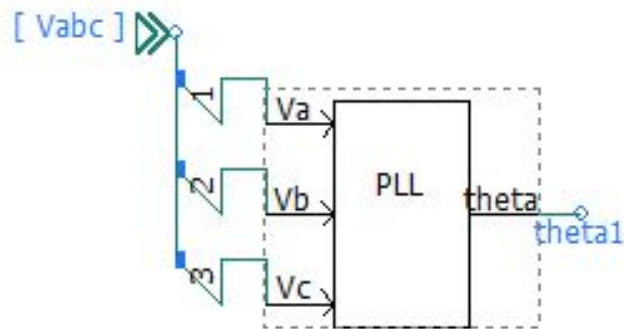


Figure 3.12: Power circuit diagram in PSCAD simulator shows the phase locked loop that are used to track the grid voltage.

the function of the PLL since it should work in harmony with the grid. It must phase lock its internal oscillator to some certain power signal from grid to generate an amplitude and phase coherent internal signal, which is used for control system. PLL produces continuous information about the phase angle and amplitude of the magnitude of interest such as grid voltage that allows space vector based controller to be employed. PLL mainly consists of three main block as shown in fig3.14. The first block is the phase detector PD, which generates an output signal relative to the phase difference between the signal generated by the oscillator and the input signal. The second block is the loop filter LF, which provides a low pass filtering to the high frequency AC signal from PD block. PI controller or first order low pass filter can be employed for this block. The third block is the volatge controlled oscillator VCO, which generates with its output an AC signal that has shifted frequency based on the given central frequency [16].

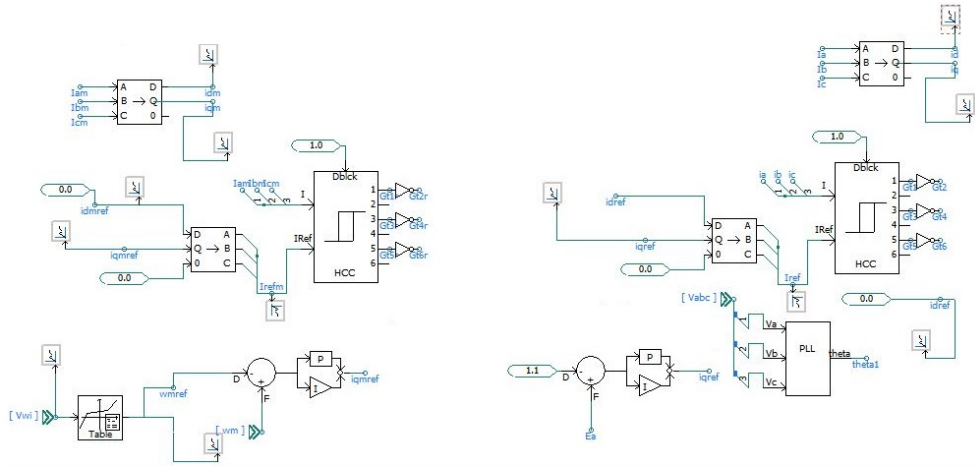


Figure 3.13: Power circuit diagram in PSCAD simulator shows 2-level inverters, 2-level rectifier and the control system for both the rectifier and the inverter.

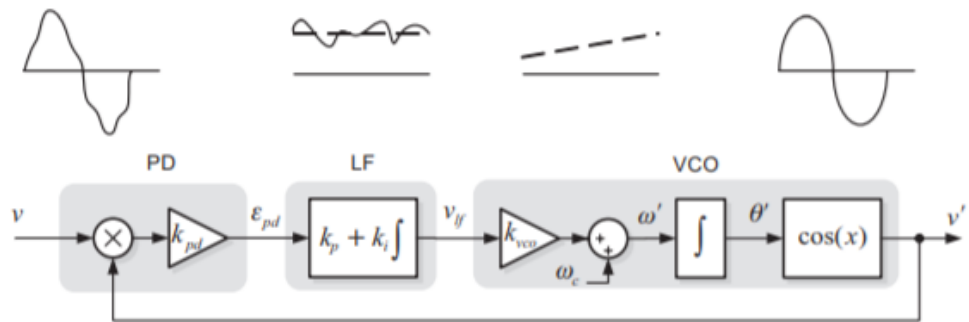


Figure 3.14: The structure of the phase locked loop PLL [16].

### 3.3.3 Output power control

The extracted power from the wind turbine can be controlled in order to optimize the power by several control strategies. Pitch control and passive stall control are the most popular control strategies being used to optimize the extracted power from the wind turbine. Pitch controller is equipped with a closed loop rotor speed controller that regulates the pitch angle for the rotor blades in order to optimize the extracted mechanical power from the turbine with respect to the wind speed variation [26]. Therefore, the rotor blades will be either pitched toward the wind to optimize the wind energy or turned out the wind to protect the turbine from the mechanical damage. In addition, while the wind speed ranges from cut-in speed to the nominal speed, the power coefficient  $C_p$  will be optimized by adjusting the pitch angle, which results to maximize the output power from the turbine. For the high wind speeds, the pitch controller will maintain a constant nominal power. The other control strategy is the passive stall control, which is aerodynamically designed to produce turbulence beyond a certain speed and gradually increasing the attack's angle of the blades until leading the blades to stall [24]. For high wind speed, this topology allows regulating the mechanical power from the wind turbine to protect it from any mechanical damages. Moreover, the pitch angle is constant, which results to low maintenance cost compared to pitch control strategy, because the less mechanically moving elements [23]. However, the disadvantage of this control topology is during

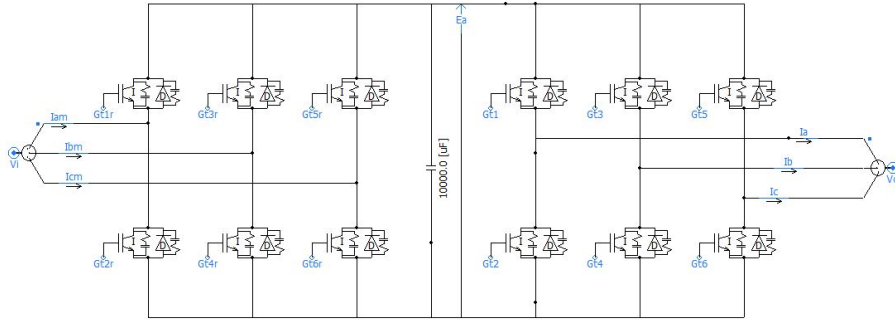


Figure 3.15: Power circuit diagram in PSCAD simulator shows the 2-level converter used for rotor side and grid side.

the operating speeds above the nominal wind speeds, which leads to drop in below the nominal power. Furthermore, another disadvantage is the voltage flicker in the system since the turbine torque is sensitive to any change in the wind speed [15]. The control model for the converters that are used in this model consists of two levels converters for the rotor side and the grid side converters. In addition, it is developed based on IGBT switches as illustrated in fig3.15.

### 3.4 Water desalination plant

Water desalination process is an intensive energy consumption, which results to high cost. Thermal process such as multistage flash (MSF) requires thermal and electrical energy such as heaters and pumps for water desalination process. It requires the electrical energy for driving the pumps such as water cooling pumps, water recycling pumps and brine blow down pumps [28]. It mainly consumes between  $19.58 \text{ kWh}/m^3$  and  $27.25 \text{ kWh}/m^3$  to desalinated water. On the other hand, reverse osmosis (RO)

requires electrical energy for the high pressure pumps, which consumes about 4-6 kWh/ $m^3$ , which make it widely used in many of the desalination plants [2].

The minimum energy requirement for water desalination can be expressed by using Van't Hoff formula as following:

$$\pi = cRT, \quad (3.3)$$

Where,  $\pi$  the osmotic pressure,  $c$  the molar concentration of salt ions,  $R$  the gas constant, which equals 0.082 and  $T$  the ambient temperature on the absolute temperature scale. For the seawater,  $c$  equals 1.128 mol/liter, which results the  $\pi$  to be 27.8 bar or 278 kg.m/L. Moreover, since each 10 Joules equal 1 kg.m or 0.77 kWh/ $m^3$ . In this model, the grid in the PSCAD simulator represents the water desalination plant since the inverter's controller requires the angle  $\theta$  for voltage synchronization.

### 3.5 Simulation results and discussion

A single wind turbine with power conversion system is modeled and simulated in PSCAD simulator as illustrated in fig3.7 with a simulation time step of  $50\mu s$ , which is a typical step for most practical circuits. In addition, this simulation time step allows high accuracy for the waveform of the system output and power electronics converter [46]. Simulation time steps can be changed to different values to get more accuracy but with a long simulation time [47]. In this scenario, the rectifier maintain

the output voltage of the PMSG, while the inverter maintain the output active power. To simulate the the entire system with the grid, six turbine units of 2 MW connected in parallel with the grid and simulated as shown in fig3.16a. Each wind turbine has own transformer in order to connect the turbine with the grid, which is step up transformer and the grid voltage level is 13.2 kV. In order to illustrates the effect of speed changes on the turbine, the wind speed suddenly decreases from 9.5 m/s to 7.5 m/s at 20s simulation time. Fig3.22 shows the output voltage of the rectifier, which maintains the voltage at 1.1 pu. While the wind speed suddenly decreases from 9.5 m/s to 7.5 m/s, the rectifier maintains the voltage at 1.1 pu. Fig3.23 shows the  $i_{ds}$  and  $i_{qs}$  currents of the rectifier's control system and their reference respectively. Similarly, fig3.24 show the inverter's actual and reference current components  $I_q$  and  $I_d$  respectively.  $I_q$  is regulated to maintain the output active power of the turbine since the  $I_d$  current is set to be zero. Moreover, Fig3.18 shows the output active and reactive powers from one turbine, which equal approximately 1.89 pu active power and approximately 0.05 pu reactive power. When the wind speed suddenly changed, the output active power drops to 0.65 pu and the reactive power drops to 0.01 pu since the active power depends on the wind speed. In addition, fig3.19 shows the total output active and reactive powers from six wind turbine  $P_T$  and  $Q_T$  to the grid.

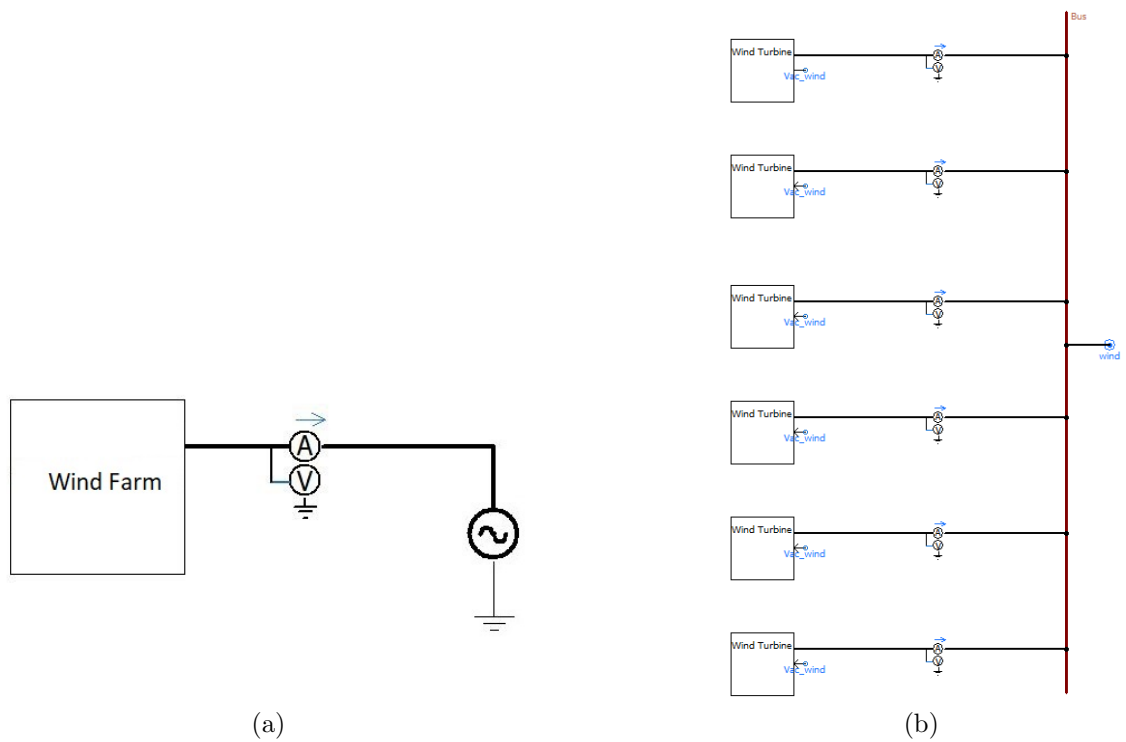


Figure 3.16: (a) Overall Schematic diagram in PSCAD for wind farm connected with the grid, (b) Detail schematic inside the wind farm showing six wind turbine units connected in parallel with total of 12 MW. The detail model of each unit is illustrated in fig 3.7 .

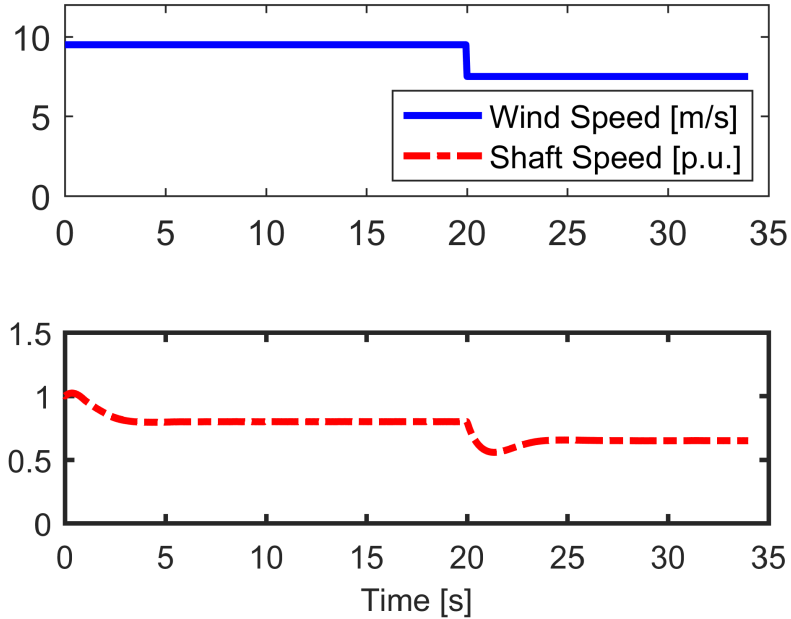


Figure 3.17: The wind speed and the mechanical speed of the generator, where the mechanical speed equal 0.8 p.u. at wind speed 9.5 m/s and drops to 0.65 p.u. when the wind speed suddenly changed.

### 3.6 Summary

This chapter explains the layout of a multi wind turbines grid connected model built in PSCAD, which is a simulation software typically employed for power system transient analysis. The system consists of six wind turbines with their own rectifier, inverter, control system for both rectifier and inverter and step up transformer. Each wind turbines rated of two MW with total of 12 MW of the entire wind turbines. All sections are connected in parallel. For the grid side inverters, the grid voltage oriented control VOC is used, which allowing independent control of active and reactive

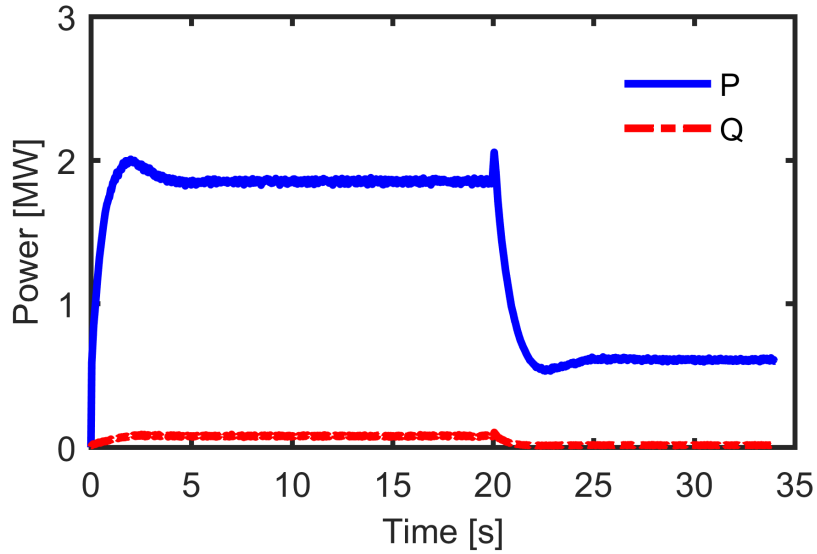


Figure 3.18: The output active and reactive powers from one wind turbine, where numeric change happens in the first second and then being regulated by the controller. When the wind speed suddenly changed, the output active power drops to 0.65 pu and the reactive power drops to 0.01 pu since the active power depends on the wind speed.

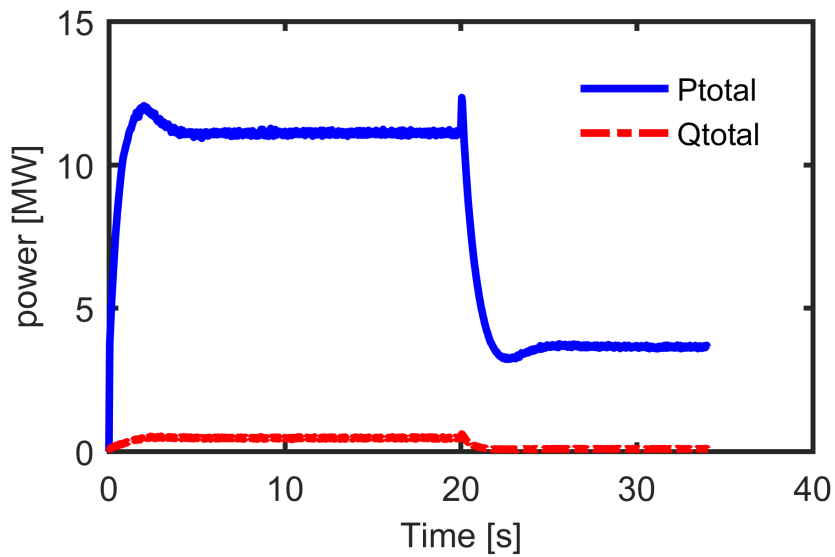


Figure 3.19: The total output active and reactive powers from six wind turbine to the grid.

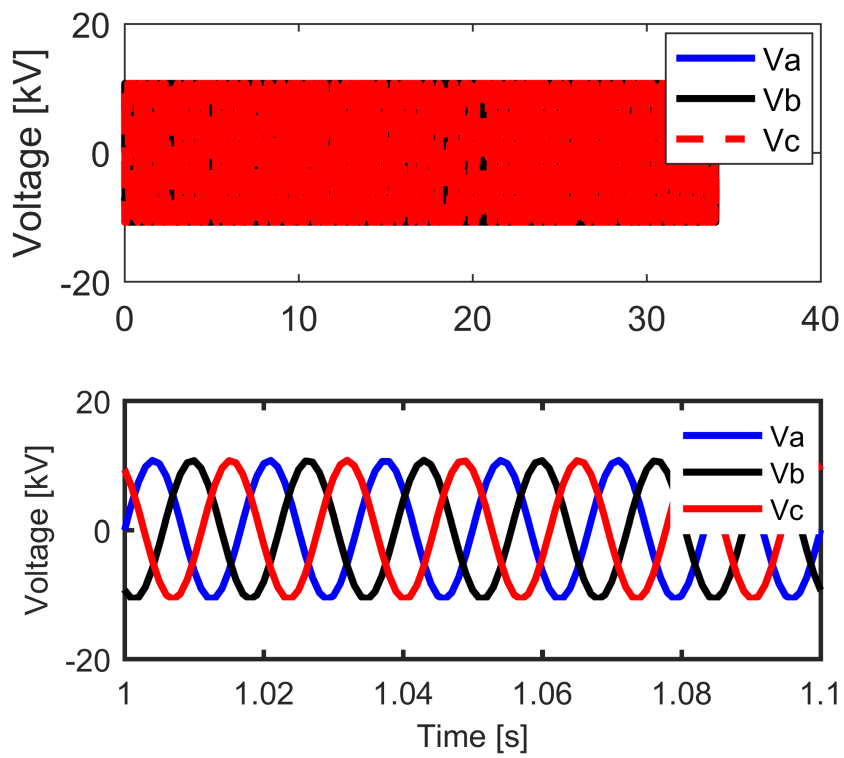


Figure 3.20: The three phase output voltages from six wind turbines.

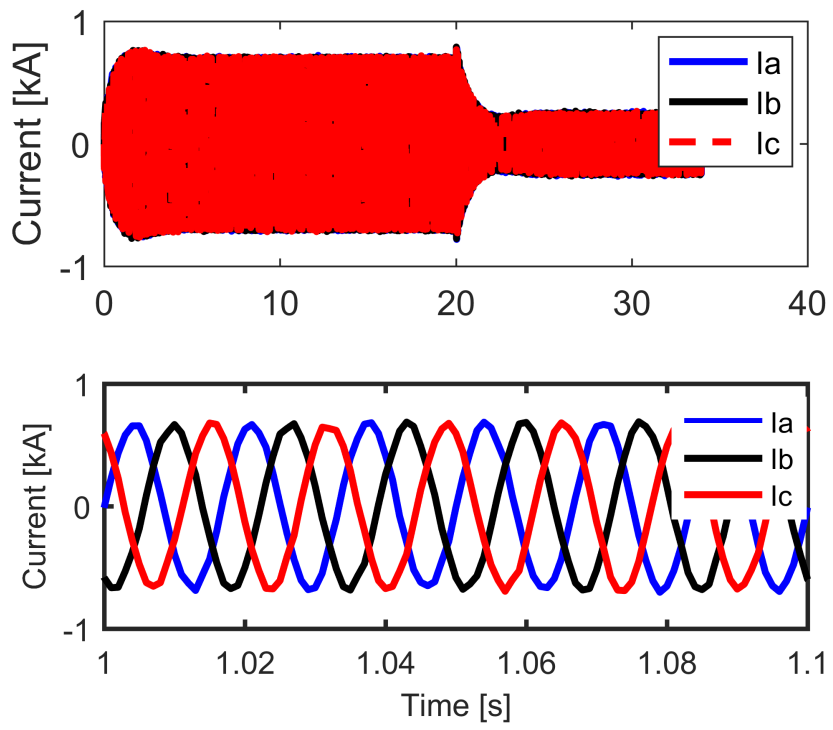


Figure 3.21: The three phase output currents from six turbines, where it decreases when the wind speed decrease.

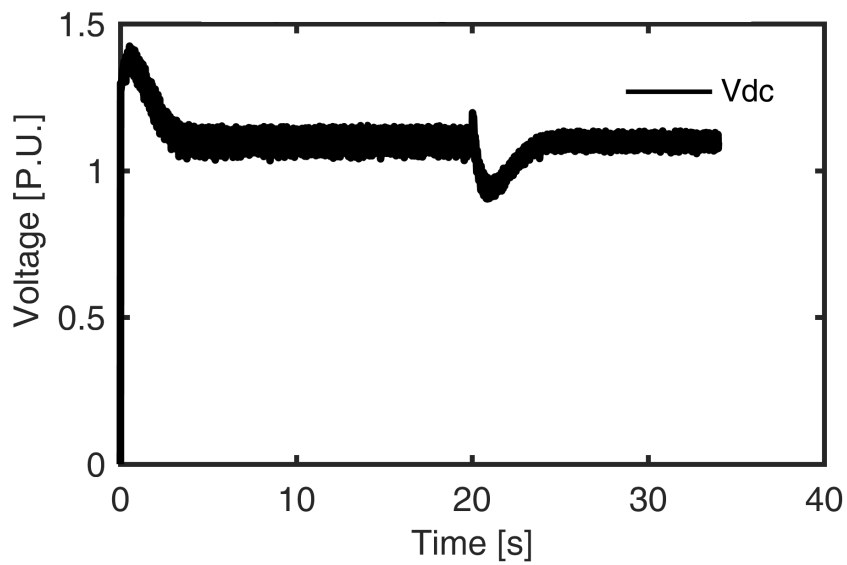


Figure 3.22: The output voltage of the rectifier, which maintains the voltage at 1.1 kV. While the wind speed suddenly decreases from 9.5 m/s to 7.5 m/s at 20s, the rectifier maintains the voltage at at the same value with a numeric change due to the change in  $I_q$ .

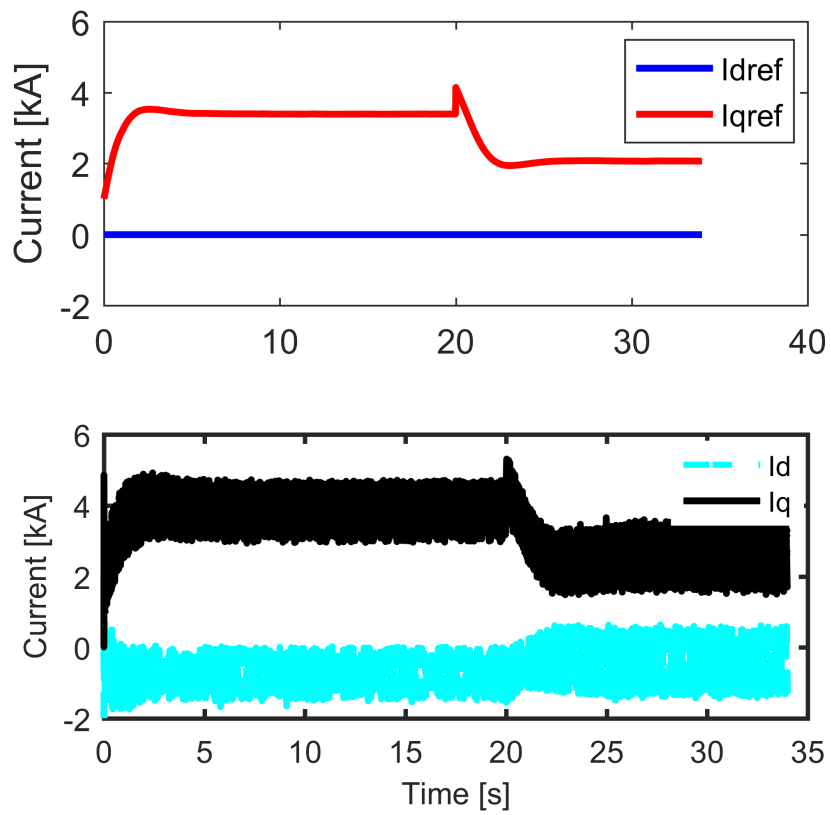


Figure 3.23: The  $I_d$ ,  $I_q$  and their reference currents for the controller of rectifier, where the  $I_d$  is set to be zero and the  $I_q$  is regulated to maintain the voltage at reference value.

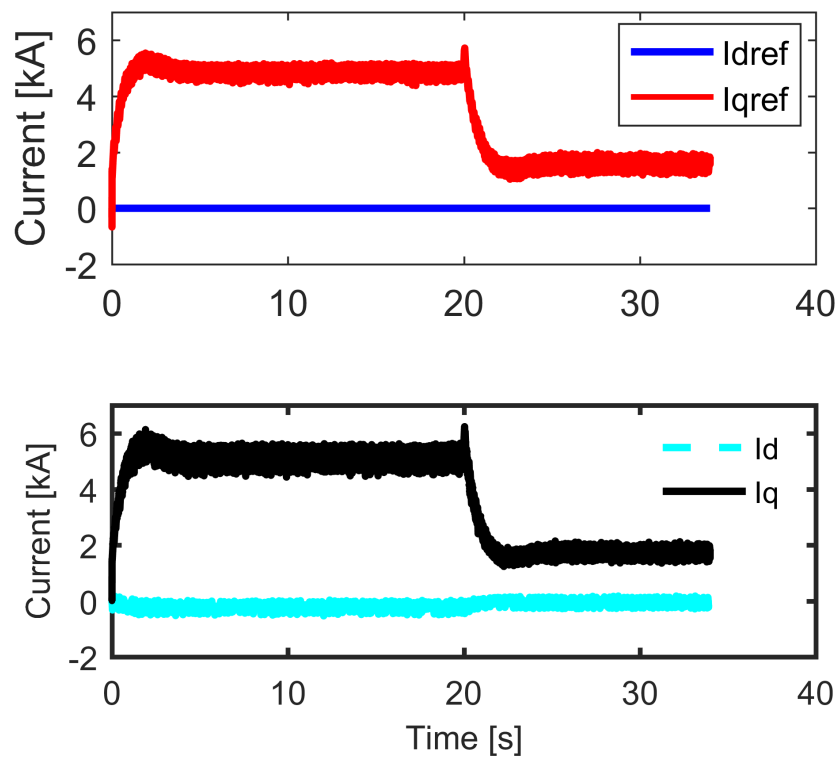


Figure 3.24: The  $I_d$ ,  $I_q$  and their reference currents for the controller of inverter, where the  $I_d$  is set to be zero and the  $I_q$  is regulated to maintain the active power.

powers. In addition, the grid-side converter controls the DC bus voltage and the reactive power, while the generator-side converter controls active powers by controlling the currents of the rotor circuit. The control topology of the converters is zero  $d$ -axis control (ZDC), where the  $d$ -axis reference current of the stator is kept zero and the stator current equal the  $q$ -axis stator current  $i_{qs}$ .

# Chapter 4

## Case Studies for Desalination Plant Integrated with Hybrid Power System

### 4.1 Introduction

Using renewable energy resource for electricity generation became trend in many countries in the world. In addition, renewable energy resources can be used for several purposes such as water desalination, transportation and water cooling and heating. Furthermore, renewable energy resources could be used to provide electricity to the rural areas, which struggle from the power outages due to the unavailability of the power resources [19]. The potentials in wind power as well as PV systems have been growing significantly in the last decade. Many countries started to build wind farms and integrate them with their grid and with other renewable energy resources such as PV. For instance, the united states plans to receive 20 percent of their power demand from the from wind by 2030. In addition, Saudi Arabia plans to produce

200 GW from the renewable energy resources by 2030 [4]. Solar energy is one of the most attractive resource of renewable energy, because it is scalable for residential and multi-megawatts installations. Also, it can meet most of the power requirements [42].

## 4.2 Overall rating

The first proposed model consists of 6 individual wind turbines of 2 MW, which total of 12 MW and 1.5 MW from PV unit is integrated with grid, which represents the desalination plant as illustrates in fig4.3. For PV system, the PSCAD model, PV arrays and the control systems was developed by one of the SPARK's lab member Mr. Akeyo in partial fulfillment of the requirements for his master degree as shown in fig4.2. The open circuit voltage of PV module counts on the material used for the cell, which is between 23.3 to 44.2 V [34]. Therefore, in this module, 2 parallel strings with 40 cells connected in series per strings to have an open circuit voltage of 43.7 V and short circuit current of 9.12 A for each module under standard test conditions (STC). The PV array consists of 160 strings with 24 modules in each strings connected in series in order to regulate the DC voltage to be under 1 kV [55]. In addition, the PV array suddenly shaded in order to illustrates the effect of irradiance drop. In this case study, the irradiance dropped from 1000 W/m<sup>2</sup> to 500 W/m<sup>2</sup> at 20s simulation time as well as the wind speed dropped from 9.5 m/s to 7.5 m/s at the same simulation time. The change in the wind speed leads to a decrease in the output active power

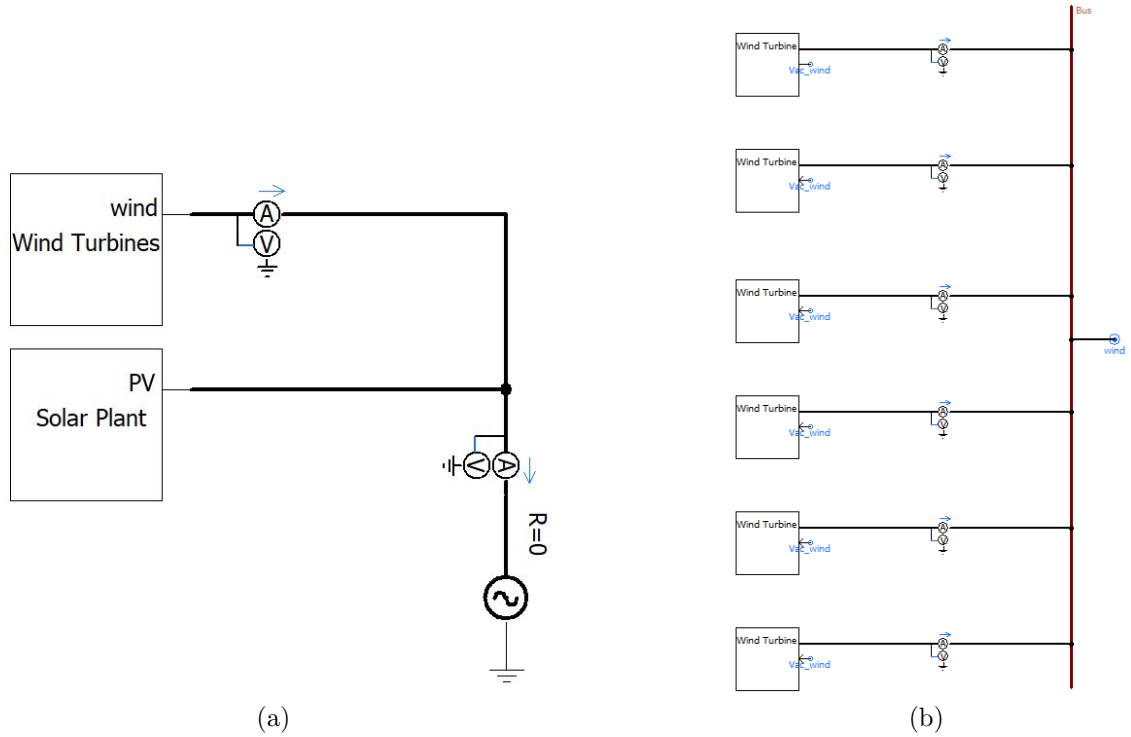


Figure 4.1: (a) Schematic of the system in PSCAD showing the wind farm connected in parallel with 1 MW solar plant, (b) Six wind turbine units connected in parallel with total of 12 MW.

of the turbine following which the inverter reduces its  $i_q$  reference. Similarly, the DC bus voltage of the PV decreases, because the PV inverter reduces its real power reference to compensate for the shading. In addition, when the irradiance suddenly reduced, the array terminal voltage moves away from the MPP before the controller adjusts the duty cycle ratio and then back at MPP.

The second proposed model consists of six wind turbines with total of 12 MW connected in parallel and works as stand alone system for a R-L load, which represents the desalination plant. Stand alone systems are good for rural areas, which power

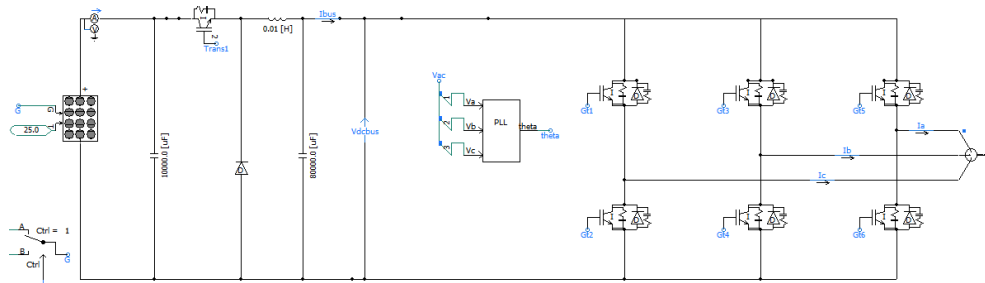


Figure 4.2: Schematic of the system in PSCAD showing the PV system with power controlling based on [9]. The detail model is illustrated in fig3.3

sources are impractical or unavailable to provide electricity. Thus, it is more economic to install a stand alone system than install a new power plant or extend the power lines and cables. In this case study, Each turbine rated of 2 MW with total of 12 MW from the six turbines. The load in the first case is R-L load, which equals  $16.66\Omega + 0.0016H$ . Fig4.16 shows the PSCAD schematic of six wind turbine units connected in parallel with R-L load.

#### 4.2.1 Simulation results

The performance of the second proposed case studies was designed and simulated at  $50\mu s$  solution time-step using PSCADTM/ EMTDCTM. The system works as stand alone mode, which an arbitrary rotating reference frame at 60 Hz is used. Also, the  $I_d$  current is forced to be zero and the  $I_q$  current controls the active power of the turbine as shown in fig4.13. In addition, the absorbed reactive power depends on the load inductance. The output power from the wind turbine is operating at maximum power point. At 20s simulation time, wind speed dropped from 9.5 m/s to 7.5 m/s

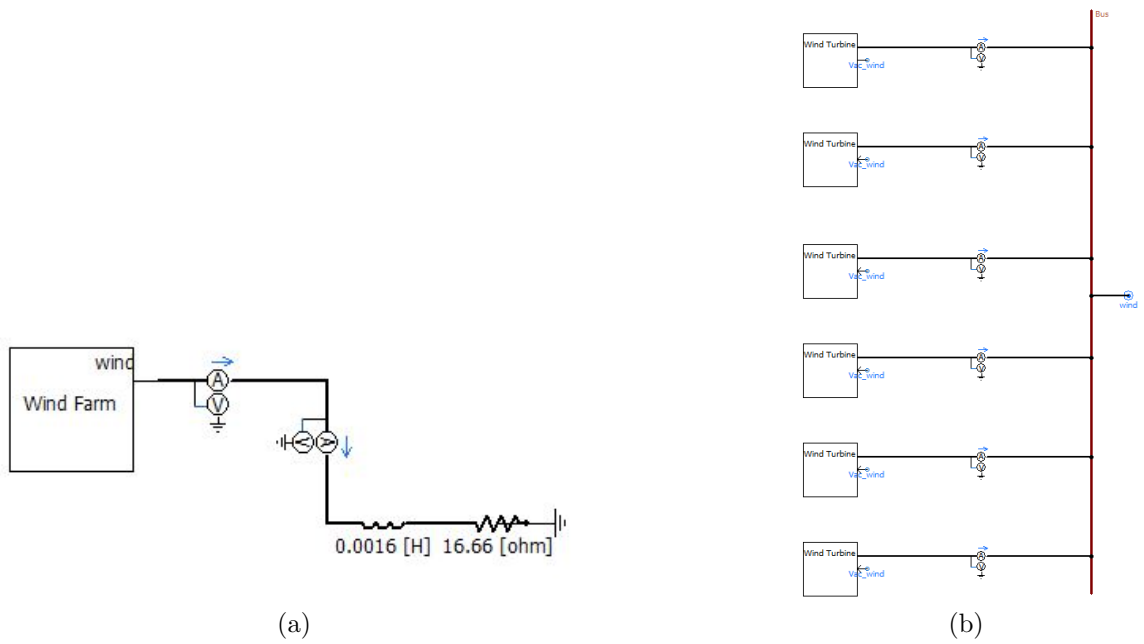


Figure 4.3: (a) Schematic of the system in PSCAD showing the load connected with the wind farm, which consists of 6 wind turbines connected in parallel with total of 12 MW, (b) Six wind turbine units connected in parallel with total of 12 MW.

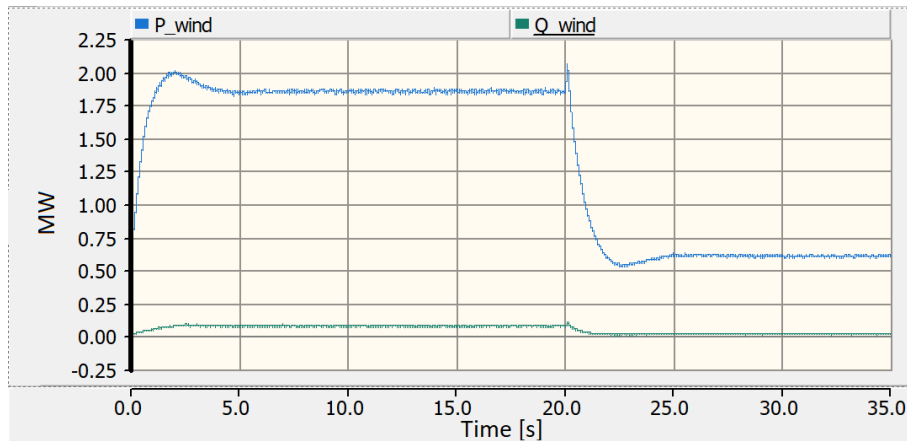


Figure 4.4: The output active and reactive powers from one wind turbine, where numeric change happens in the first second and then being regulated by the controller. When the wind speed suddenly changed, the output active power drops to 0.65 pu and the reactive power drops to 0.01 pu since the active power depends on the wind speed.

in order to illustrates the effect of the wind speed changes on the system.

The output reactive power of the system should be zero. However, since the load in the stand alone system is R-L load and the voltage equations of the PMSG as illustrated in equations 2.21 and 2.22 in chapter 2 shows that the  $V_d$  is not zero even  $I_d$  is zero. Therefore, the reactive power of the system  $Q = \frac{3}{2} I_q V_d$ . In addition, the angle of the grid  $\theta$  is required for transformation and is obtained from a synchronous rotating reference frame at 60 Hz.

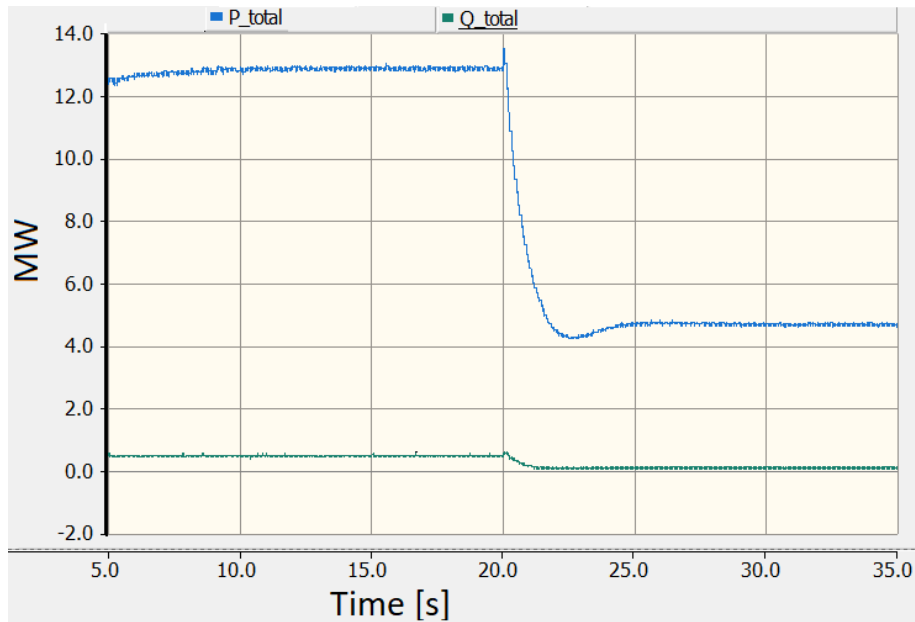


Figure 4.5: The output active and reactive powers from six wind turbines and PV system, where numeric change happens in the first second and then being regulated by the controller. When the wind speed suddenly changed, the output active power drops to 5 MW and the reactive power drops to 0.01 pu since the active power depends on the wind speed.

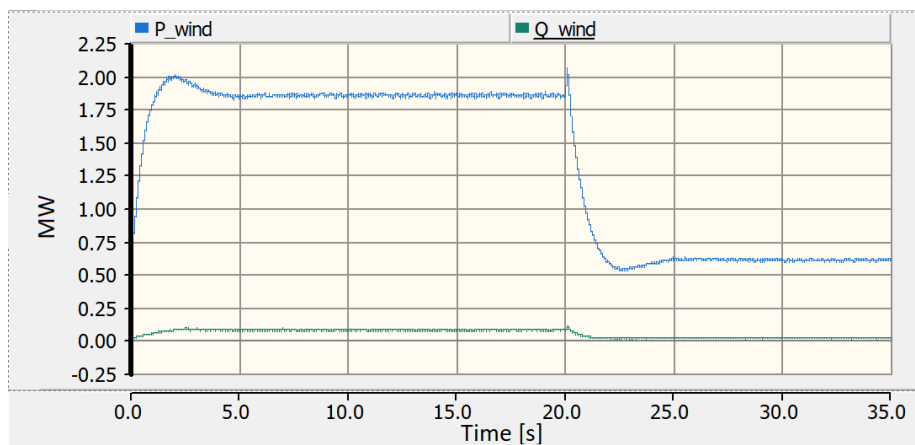


Figure 4.6: The output active and reactive powers from one wind turbine, where numeric change happens in the first second and then being regulated by the controller. When the wind speed suddenly changed, the output active power drops to 0.65 pu and the reactive power drops to 0.01 pu since the active power depends on the wind speed.

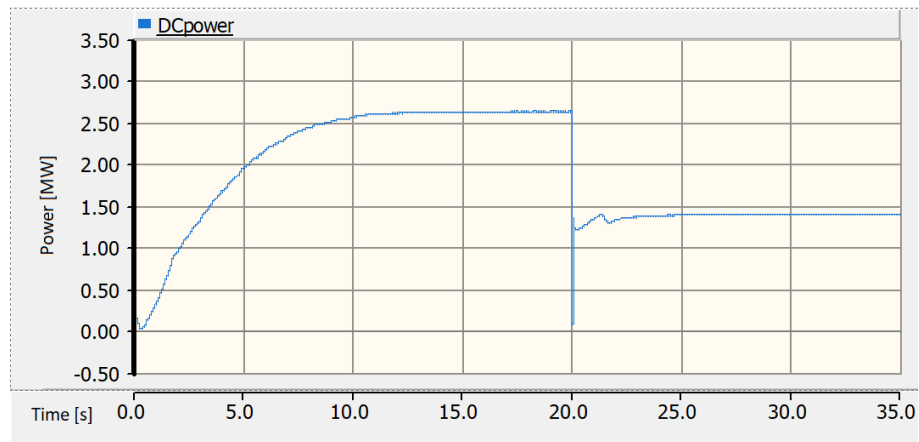


Figure 4.7: The DC Power from the PV. Reduction in irradiance at 20s simulation time leads to decrease in PV output current making the PV DC power drop.

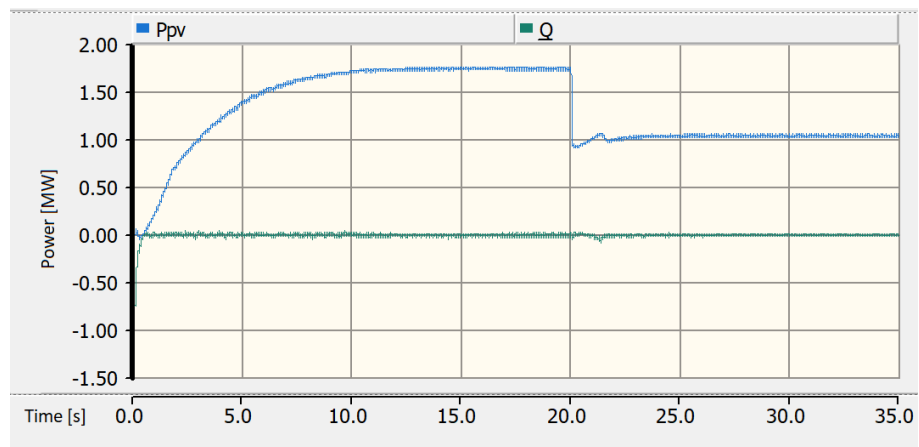


Figure 4.8: PV AC power output at unity power factor irrespective of changes in array irradiance..

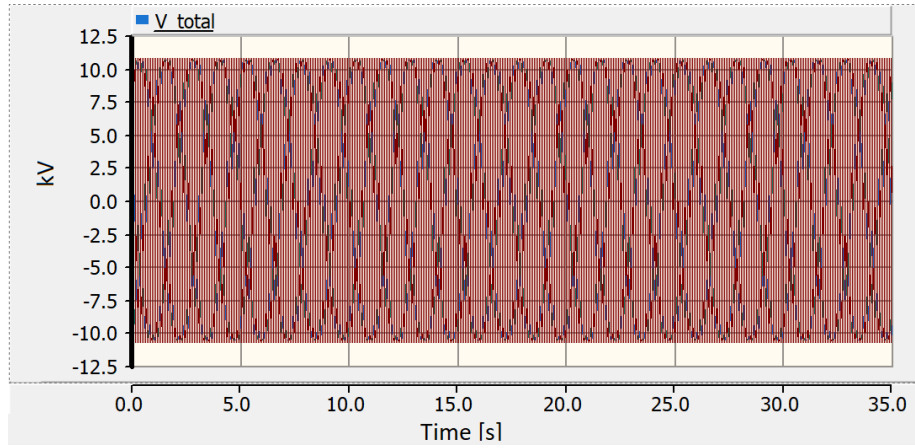


Figure 4.9: The three phase output voltages of the system.

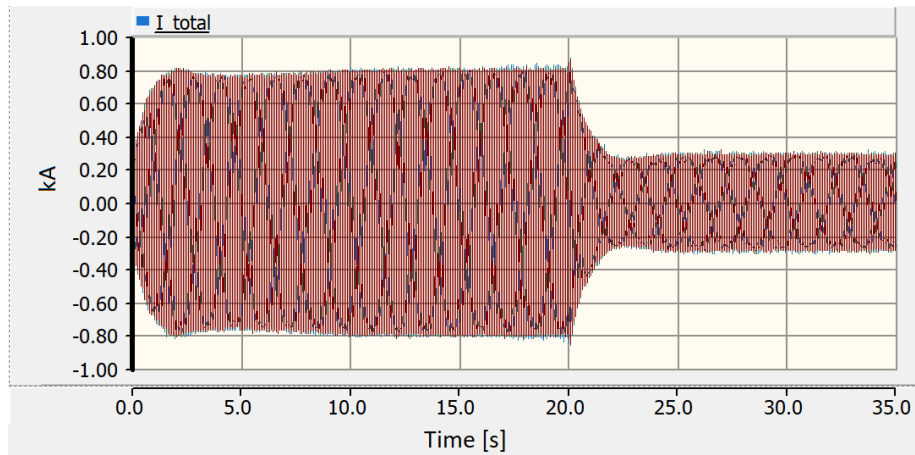


Figure 4.10: The three phase output currents to the grid.

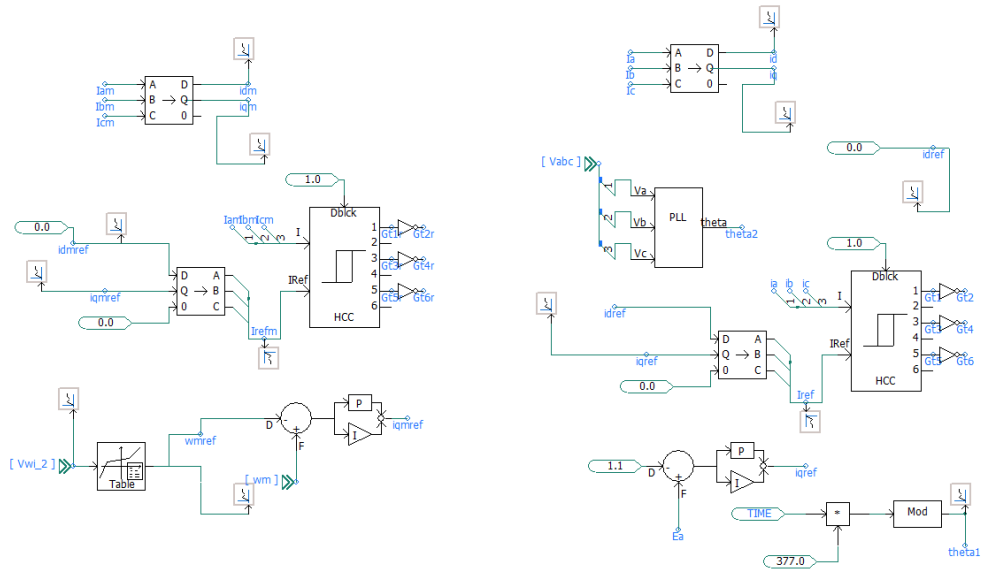


Figure 4.11: The control system of the power conversion system of the wind turbine operating in the stand-alone mode.

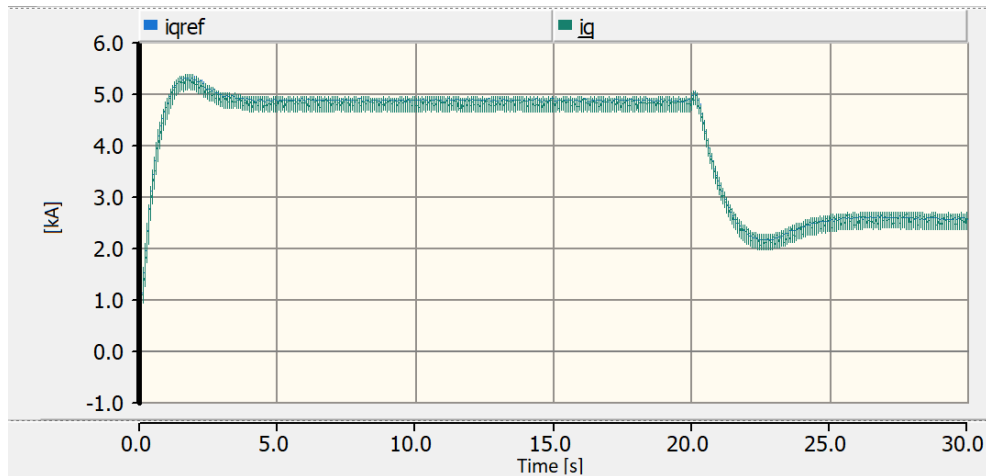


Figure 4.12: The  $I_q$  current and its reference current for the controller of inverter, where the  $I_d$  is set to be zero and the  $I_q$  is regulated to maintain the active power. The magnitude of the  $I_q$  current is high, because the rating of the system, where the control is being difficult for high ratings.

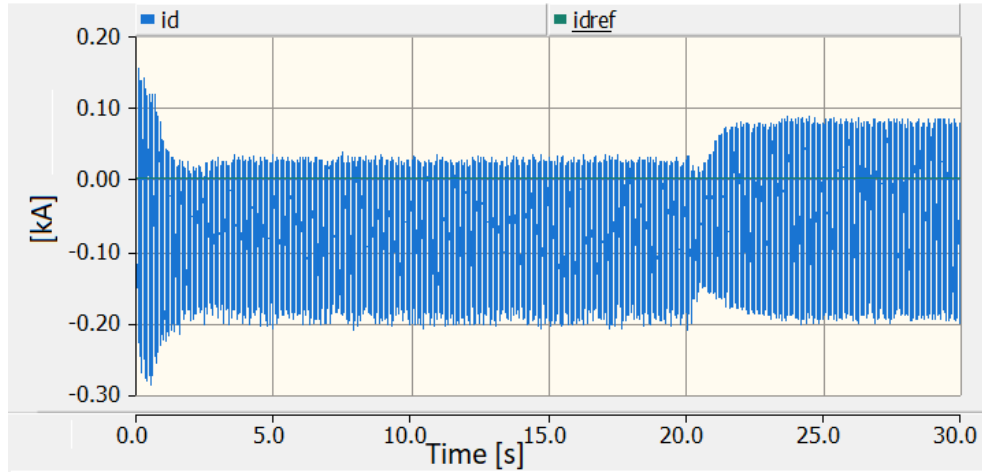


Figure 4.13: The  $I_d$  current and its reference current for the controller of inverter, where is set to be zero and the. The high ripple is a result of the PI tuning of the controller and the high rating of the system.

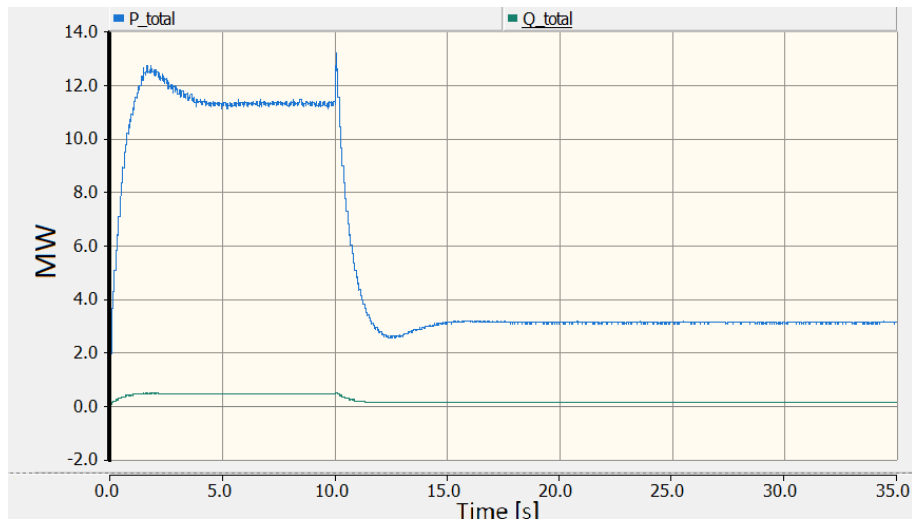


Figure 4.14: The output active and reactive powers from the system, where numeric change happens in the first second and then being regulated by the controller. When the wind speed and the irradiance suddenly changed, the output active power drops to 5.1 MW and the reactive power drops to 0.01 pu since the active power depends on the wind speed.

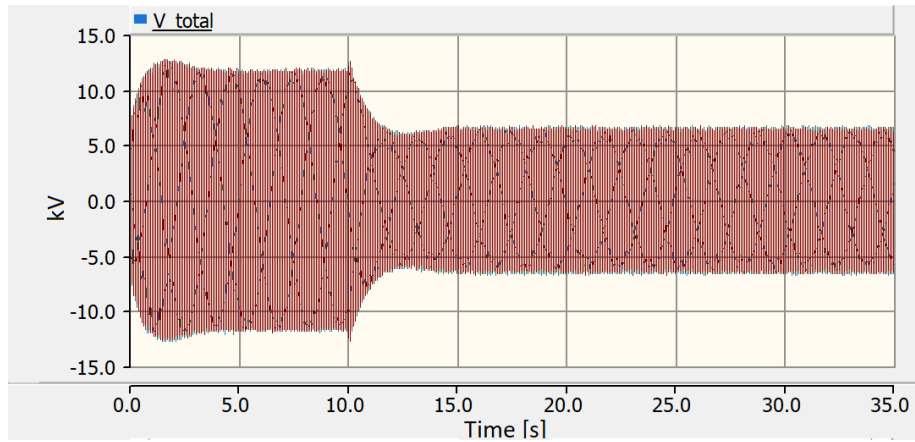


Figure 4.15: Schematic of the system in PSCAD showing the wind farm connected in parallel with solar plant. The wind farm consists of 6 wind turbine units connected in parallel with total of 12 MW and the PV rated of 1 MW.

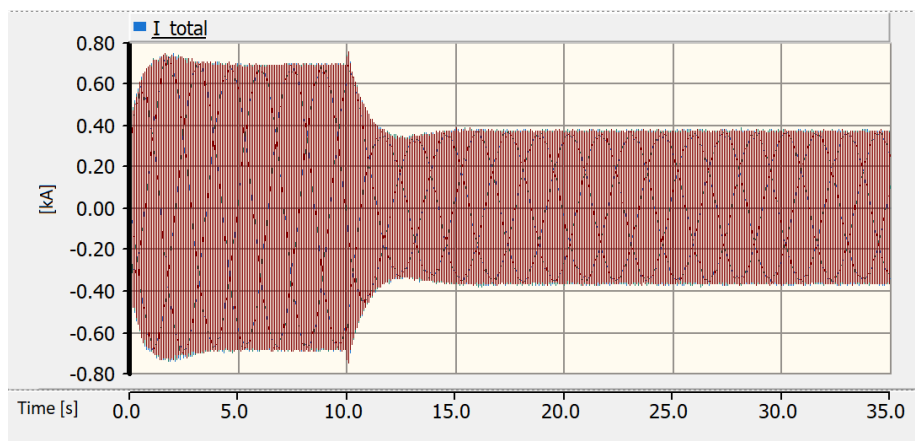


Figure 4.16: Schematic of the system in PSCAD showing the wind farm connected in parallel with solar plant. The wind farm consists of 6 wind turbine units connected in parallel with total of 12 MW and the PV rated of 1 MW.

# Chapter 5

## Conclusions and Future Work

### 5.1 Conclusions

This thesis focus on integrating a multi-wind turbine units connected in parallel with the grid. The output power from the wind farm to the grid was controlled under different wind speeds. Also, a PV system and wind farm which consists of 6 wind turbine units connected in parallel integrated with the grid was simulated and analyzed. The power control of both PV system and wind turbines under several conditions such as wind speeds variation and irradiance variations was simulated and analyzed. In addition, the wind farm connected with the load and work as a stand alone system, which represents the water desalination plant was introduced and simulated. The wind blades, permanent magnet synchronous generator, power electronic converters, controls and transformers were designed and simulated using *PSCAD<sup>TM</sup>/EMTDC<sup>TM</sup>*, which is a tool typically employed for power system transient analysis.

In chapter 1 and 2, background about the research and relevant topics were reviewed as well as modeling of components and different control strategies for the power system conversion. Also, the water desalination process and power consumption were introduced.

In chapter 3, a significant concept and software implementation of 12 MW wind farm integrated with the grid was introduced. The wind farm consists of 6 wind turbine units rated of 2 MW connected in parallel with total of 12 MW. Each turbine has its own PMSG, power conversion system and control and step up transformer.

In chapter 4, two different case studies were implemented and introduced. The first one was a grid tied wind farm and PV system with different environment conditions such as wind speed change and irradiance changes. The control system of the power conversion regulates and maintain the voltage and the output active power. The other case study was a stand alone system, which integrate the wind farm with load that represent water desalination plant.

## **5.2 Future work**

The thesis has explained integrating different renewable energy resources with the grid along with associated control scheme under several environment conditions. Extract the maximum power from the turbine can be achieved by several control strategies such as pitch control and aerodynamic design of the blades. Pitch control strategy maintains the optimal power from the turbine over a wide range of wind speed

conditions. Pitch control maintains the actual output power of the generator to be around the rated power by increasing the pitch angle when the wind speed exceeds the rated speed of the turbine. Thus, the mechanical and electrical components of the turbine such as the generator and the blades could be protected for over-wind speed conditions. In addition, future work can investigate the transient and sub-transient of stand alone systems integrated with wind farm and PV system. Also simulate and analyze the effect of the relative wind turbine size, and control strategies employed on the stability of the grid in case of wind speed exceeds the rated speed.

# References

- [1] “Wind energy data,” Jul 2015. [Online]. Available: <http://resourceirena.irena.org/gateway/dashboard/>
- [2] P. Tewari, “Desalination and water purification technologies,” *Government of India department of atomic energy*, vol. 1, no. 13, pp. 39–46, Nov 2010.
- [3] T. Younos, “Solar photovoltaic and thermal energy systems: current technology and future trends,” *Contemporary water research and education*, vol. 132, no. 13, pp. 39–46, Nov 2015.
- [4] V. Vekhande, N. Kothari, and B. G. Fernandes, “Vision 2030 and the birth of saudi solar energy,” *Middle East Institute Policy Focus Series*, pp. 8–19, Jul 2016.
- [5] G. Velasco-Quesada, F. Guinjoan-Gispert, R. Pique-Lopez, M. Roman-Lumbreras, and A. Conesa-Roca, “Electrical pv array reconfiguration strategy for energy extraction improvement in grid-connected PV systems,” *IEEE Transactions on Industrial Electronics*, vol. 56, no. 11, pp. 4319–4331, Nov 2009.
- [6] Y. Yang and F. Blaabjerg, “Overview of single-phase grid-connected photovoltaic systems,” *Electric Power Components and Systems*, vol. 43, no. 12, pp. 1352–1363, 2015.
- [7] I. H. Mahammed, Y. Bakelli, S. H. Oudjana, A. H. Arab, and S. Berrah, “Optimal

- model selection for pv module modeling,” in *2012 24th International Conference on Microelectronics (ICM)*, Dec 2012, pp. 1–4.
- [8] M. Z. Daud, A. Mohamed, M. Z. C. Wanik, and M. A. Hannan, “Performance evaluation of grid-connected photovoltaic system with battery energy storage,” in *Power and Energy (PECon), 2012 IEEE International Conference on*, Dec 2012, pp. 337–342.
- [9] O. Akeyo, “Analysis and simulation of photovoltaic systems incorporating battery energy storage,” *Master Thesis*, p. 41, Sep 2017.
- [10] J. H. R. Enslin, M. S. Wolf, D. B. Snyman, and W. Swiegers, “Integrated photovoltaic maximum power point tracking converter,” *IEEE Transactions on Industrial Electronics*, vol. 44, no. 6, pp. 769–773, Dec 1997.
- [11] M. S. M. Moh and N. Asmuin, “Comparison of horizontal axis wind turbines and vertical axis wind turbines,” *IOSR Journal of Engineering*, vol. 04, no. 08, pp. 27–30, Aug 2014.
- [12] M. S. R. Marwan and N. Asmuin, “Development of phasor type model of pmsg based wind farm for dynamic simulation analysis,” *IEEE Transactions on Industry Applications*, vol. 11, no. 08, pp. 271–295, Aug 2014.
- [13] S. M. R. Marwan and T. Rion, “New controller design for pmsg based wind generator with lcl-filter considered,” *2012 International Conference on Electrical Machines*, vol. 10, no. 08, pp. 2110–2116, Sep 2012.
- [14] R. Marwan and T. Murata, “Stability augmentation of a grid connected wind farm,” *Green Energy and Technology*, May 2009.
- [15] R. Teodorescu, M. Liserre, and P. Rodriguez, *Introduction*. Wiley-IEEE Press,

- 2011, pp. 1–4. [Online]. Available: <http://ieeexplore.ieee.org.ezproxy.uky.edu/xpl/articleDetails.jsp?arnumber=5732936>
- [16] L. M. T. Remus and R. Pedro, in *Grid Converters For Photovoltaic and Wind Power Systems*, vol. 1, Feb 2011, pp. 51–66.
- [17] H. A. A. Shahrouz and A. Jrn, “A review of renewable energy supply and energy efficiency technologies,” *IEEE Transactions on Power Electronics*, vol. 8145, no. 1, pp. 998–1009, April 2014.
- [18] A. N. Kh, “Renewable energy types,” *Journal of Clean Energy Technologies*, vol. 2, no. 1, pp. 61–77, April 2014.
- [19] K. Ma and F. Blaabjerg, “Wind energy systems,” *Proceedings of the IEEE*, vol. 105, no. 11, pp. 2116–2131, Nov 2017.
- [20] —, “Solar photovoltaic and thermal energy systems: current technology and future trends,” *Proceedings of the IEEE*, vol. 105, no. 11, pp. 2133–2155, Nov 2017.
- [21] M. M. H. Abu-Rub and K. Alhaddad, in *Power Electronics for Renewable Energy Systems, Transportation and Industrial Applications*, vol. 1, Feb 2014, pp. 2–15.
- [22] W. Xudong and X. Honglun, “Shape design and aerodynamic characteristics of wind turbine blades based on energy cost,” *2015 Seventh International Conference on Measuring Technology and Mechatronics Automation*, vol. 105, no. 11, pp. 973–994, Sep 2015.
- [23] Z. Wu and D. Yang, “Comprehensive modeling and analysis of permanent magnet synchronous generator wind turbine system with enhanced low voltage ride through capability,” *2015 Seventh International Conference on Measuring Technology and Mechatronics Automation*, vol. 105, no. 11, pp. 455–494, Sep 2012.

- [24] X. L. L. Zhang and Y. Sun, "Design on pitch-control wind turbine system based on bladed," *Control and Decision Conference*, vol. 105, no. 11, pp. 3921–3956, Aug 2011.
- [25] P. Dvorak and K. Hruska, "Optimization of a pmsm design for control with zero direct axis current component," *Proceedings of the IEEE*, vol. 105, no. 11, pp. 162–169, Jul 2016.
- [26] O. M. K. Saleh and M. Badr, "Field-oriented vector control of synchronous motors with additional field winding," *IEEE Transactions on Energy Conversion*, vol. 19, no. 1, pp. 95–101, Feb 2004.
- [27] W. E. H. Akagi, H. and M. Aredes, in *Instantaneous Power Theory and Applications to Power Conditioning*, vol. 1, March 2007, pp. 41–49.
- [28] O. Buros, "The abcs of desalting," *International Desalination Association*, vol. 1, no. 13, pp. 31–36, Aug 2000.
- [29] R. D. Doncker, D. W. Pulle, and V. Andre, *Advanced Electrical Drives Analysis, Modeling, Control*. Springer Netherlands, 2011.
- [30] E. S.-T. Importados), *Power Electronics Handbook - 3 Ed.* Elsevier (St-Tecnico Importados), 2011.
- [31] A. Sangwongwanich, Y. Yang, and F. Blaabjerg, "High-performance constant power generation in grid-connected PV systems," *IEEE Transactions on Power Electronics*, vol. 31, no. 3, pp. 1822–1825, March 2016.
- [32] B. M. T. Ho, S. H. Chung, and S. Y. R. Hui, "An integrated inverter with maximum power tracking for grid-connected pv systems," in *Applied Power Electronics Conference and Exposition, 2004. APEC '04. Nineteenth Annual IEEE*, vol. 3, 2004, pp. 1559–1565 Vol.3.

- [33] K. A. Corzine, S. D. Sudhoff, and C. A. Whitcomb, "Performance characteristics of a cascaded two-level converter," *IEEE Transactions on Energy Conversion*, vol. 14, no. 3, pp. 433–439, Sep 1999.
- [34] V. Vekhande and B. G. Fernandes, "Module integrated dc-dc converter for integration of photovoltaic source with dc micro-grid," in *IECON 2012 - 38th Annual Conference on IEEE Industrial Electronics Society*, Oct 2012, pp. 5657–5662.
- [35] V. Vekhande, N. Kothari, and B. G. Fernandes, "Switching state vector selection strategies for paralleled multilevel current-fed inverter under unequal dc-link currents condition," *IEEE Transactions on Power Electronics*, vol. 30, no. 4, pp. 1998–2009, April 2015.
- [36] E. Cengelci, S. U. Sulistijo, B. O. Woo, P. Enjeti, R. Teoderescu, and F. Blaabjerg, "A new medium-voltage pwm inverter topology for adjustable-speed drives," *IEEE Transactions on Industry Applications*, vol. 35, no. 3, pp. 628–637, May 1999.
- [37] G. R. Walker and P. C. Sernia, "Cascaded dc-dc converter connection of photovoltaic modules," *IEEE Transactions on Power Electronics*, vol. 19, no. 4, pp. 1130–1139, July 2004.
- [38] W. C. C. Wang and X. le, "Modelling of a pmsg wind turbine with autonomous control," *Mathematical Problems in Engineering*, vol. 11, no. 85, p. 9, May 2014.
- [39] CEDRAT, "Wind turbine applications," *CEDRAT*, Jan 2006.
- [40] K. Sun, L. Zhang, Y. Xing, and J. M. Guerrero, "A distributed control strategy based on DC bus signaling for modular photovoltaic generation systems with battery energy storage," *IEEE Transactions on Power Electronics*, vol. 26, no. 10, pp. 3032–3045, Oct 2011.

- [41] D. P. Hohm and M. E. Ropp, “Comparative study of maximum power point tracking algorithms using an experimental, programmable, maximum power point tracking test bed,” in *Photovoltaic Specialists Conference, 2000. Conference Record of the Twenty-Eighth IEEE*, 2000, pp. 1699–1702.
- [42] S. Jain and V. Agarwal, “A single-stage grid connected inverter topology for solar PV systems with maximum power point tracking,” *IEEE Transactions on Power Electronics*, vol. 22, no. 5, pp. 1928–1940, Sept 2007.
- [43] M. Killi and S. Samanta, “Modified perturb and observe MPPT algorithm for drift avoidance in photovoltaic systems,” *IEEE Transactions on Industrial Electronics*, vol. 62, no. 9, pp. 5549–5559, Sept 2015.
- [44] W. Wareesri and S. Po-Ngam, “A three-phase PV-pump inverter with maximum power point tracking (MPPT) controller,” in *2016 13th International Conference on Electrical Engineering/Electronics, Computer, Telecommunications and Information Technology (ECTI-CON)*, June 2016, pp. 1–4.
- [45] N. Adhav, “Comparison and implementation of different pwm schemes of inverter in wind turbine,” *International Journal of Innovative Technology and Exploring Engineering*, vol. 2, no. 2, pp. 95–101, Jan 2013.
- [46] L. P. V. Jalil and V. Dinavahi, “Real-time simulation of grid-connected wind farms using physical aggregation,” *IEEE TRANSACTIONS ON INDUSTRIAL ELECTRONICS*, vol. 57, no. 9, pp. 95–101, Sep 2010.
- [47] M. H. R. Centre, “Project settings for pscad simulation,” *Manitoba HVDC Research Centre a division of Manitoba Hydro International Ltd*, vol. 57, no. 9, pp. 95–101, May 2017.

# Vita

Nasser Alawhali, Master Student

Department of Electrical and Computer Engineering, University of Kentucky

---

## EDUCATION

**Master of Science** - Electrical and Computer Engineering May 2018  
University of Kentucky

**Thesis:** Contributions to Hybrid Power Systems Incorporating  
Renewables for Water Desalination Systems

**Director of Thesis:** Dr. Dan M Ionel

**Bachelor of Science** - Electrical Engineering May 2011  
King Saud University, Riyadh, Saudi Arabia

**Dissertation:** Design and Implementation High Voltage System  
for Protection Tests

**Advisor:** Dr. Abdulrahman Alarainy

## AWARD AND RECOGNITION

Saudi Council of Engineers SCE.

## **EMPLOYMENT HISTORY**

**Academic Researcher**

King Abdulaziz City for Science and Technology

2011.07 - Present